Multimodal meta-analysis of brain integrity in disorders of consciousness

Arianna Sala[1,2,3], Michiel Meys[1,2,3], Naji Alnagger[1,3], Nikita Beliy[4], Simona Abagnale[5], Danuta Szirmai[6,7], Baris Kaan Ok[1], Zhixin Wang[1], Marjorie Bardiau[8], Charlotte Beaudart[9], Simon B. Eickhoff[10,11], Daniel Martins[12,13,14], Marco Tettamanti[15], Steven Laureys[16,17,18], Olivia Gosseries[1,3], Aurore Thibaut[1,2,3], Jitka Annen[1,2,3,19]*

[1]Coma Science Group, GIGA-Consciousness, GIGA Institute, University of Liège, Liège, Belgium
[2]NeuroRecovery Lab, GIGA-Consciousness, GIGA-Institute, University of Liège, Liège, Belgium
[3]Clinique de la Conscience et NeuroRevalidation, Department of Neurology, University Hospital of Liège, Liège, Belgium
[4]Human Imaging, GIGA-Cyclotron Research Center Human Imaging, GIGA Institute, University of Liège, Liège, Belgium
[5]IRCCS Fondazione Don Carlo Gnocchi, 50143 Florence, Italy
[6]Center for Translational Medicine, Semmelweis University, Budapest, Hungary
[7]Department of Neurosurgery and Neurointervention, Semmelweis University, Budapest, Hungary
[8]ULiège Library, University of Liège, Liège, Belgium
[9]Public Health Aging Research & Epidemiology (PHARE) Group, Research Unit in Clinical Pharmacology and Toxicology (URPC), NAmur Research Institute for LIfe Sciences (NARILIS), University of Namur, Belgium
[10]Institute of Systems Neuroscience, Medical Faculty, Heinrich Heine University Düsseldorf, Düsseldorf, Germany
[11]Institute of Neuroscience and Medicine, Brain & Behaviour (INM-7), Research Centre Jülich, Jülich, Germany
[12]Department of Neuroimaging, Institute of Psychiatry, Psychology and Neuroscience, King's College London, London, United Kingdom
[13]Department of Clinical Neurosciences and Mental Health, Faculty of Medicine, University of Porto, Portugal
[14]RISE-Health, Neurosciences Thematic Line, Faculty of Medicine, University of Porto, Porto, Portugal
[15]Department of Psychology, University of Milano-Bicocca, Milan, Italy
[16]CERVO Brain Research Centre, Laval University, Quebec, Canada
[17]Joint International Research Unit on Neuroplasticity, University of Liège, Avenue de l'hôpital 11, 4000 Liège, Belgium
[18]International Consciousness Science Institute, Hangzhou Normal University and Hangzhou Institute of Medicine of the Chinese Academy of Sciences , 2318 Yuhangtang Rd, Yuhang District, 311121 Hangzhou, Zhejiang, China
[19]Department of Data analysis, University of Ghent, Ghent, Belgium

Abstract

Disorders of consciousness represent severe neurological conditions that occur following acquired brain injury, with highly variable outcomes ranging from full recovery to prolonged unconsciousness and death. Understanding the precise brain mechanisms underlying this heterogenous group of disorders remains a scientific and medical challenge, impeding progress in the development of treatment or actionable clinical plans. Here, we sought to map the precise spatiotemporal pattern of brain alterations in these patients by performing a multimodal meta-analysis comprising 90 electroencephalography, magnetic resonance imaging and positron emission tomography studies (3,535 observations from rare patients with a prolonged disorder of consciousness and 1,372 from healthy controls). To generate hypotheses about potential underlying biological mechanisms, we quantified the spatial correspondence between brain circuits robustly associated with disorders of consciousness and openly available atlases of normative features of human brain biology, including maps on neurotransmission, which could inform new receptor-based mechanistic models of disease. By assessing 49 electrophysiological features of global brain integrity, we show that, in patients, neural electrical activity is consistently and globally stronger (i.e., spectral power and connectivity) in the delta band and weaker in the alpha band, while broadband entropy and alpha-SD of the participation coefficient best discriminate among patient groups. Using coordinate-based techniques, we identify convergent loss of structure, function and metabolism in specific cortical hubs of the default mode network and in subcortical "cognitive integration zones"[1] of the mediodorsal thalamus and of the executive caudate nucleus, at the interface between default mode and executive, salience and ventral-attention networks[2]. This convergent pattern aligns with specific receptor distributions (mGluR5, GABA-A, μ-opioid, CB1) and with the noradrenergic transporter topography, identifying putative receptor-level candidates for therapeutic trials. Altogether, our findings provide a robust foundation for refining current mechanistic models of disorders of consciousness, identifying promising clinical diagnostic biomarkers within the heterogenous literature and patient profiles, and selecting targets for therapeutic development.

Introduction

Disorders of consciousness (DoC) represent dramatic neurological conditions that occur following severe acquired brain injury leading to coma. While coma is a transient state typically lasting a few days[3], coma survivors can present highly variable outcomes ranging from full recovery of consciousness to a prolonged reduction of consciousness (minimally conscious state, MCS) or unconsciousness (unresponsive wakefulness syndrome/vegetative state, UWS/VS)[4].

Despite decades of research, the neurobiological mechanisms at the basis of prolonged DoC are far from clearly elucidated. Notwithstanding the convergence among prevailing theories of consciousness on the view that consciousness depends on the spatiotemporal *integration* of widespread patterns of brain activity[5], the discussion around the neuroanatomical basis of such neural dynamics has remained exceptionally coarse[6]. Recently, a neurobiological model for recovery of consciousness in DoC has been proposed, providing a neurobiological framework to understand the dramatic alterations in the neural signal's frequency observed in these patients[7]. Distinguishing itself from other theories[5], this mesocircuit model points at a well-specified subcortical circuit for the roots of the dysfunction underlying DoC. However, at a cortical level, it remains coarse, indicating the involvement of unspecified regions of the frontal, parietal, occipital and temporal cortices[7]. The most recent clinical guidelines for DoC[8] mirror this state of incomplete understanding of the neural mechanisms involved in DoC. While strongly recommending quantitative electroencephalography (EEG)[8] for the diagnostic work-up of DoC, no guidance is provided on which among the >250 proposed metrics of consciousness[9] provide maximal diagnostic or prognostic value. An analogous issue concerns neuroimaging assessments, such as [^{18}F]Fluorodeoxyglucose Positron Emission Tomography ([^{18}F]FDG-PET) and functional magnetic resonance imaging (fMRI), for which the guidelines fall short of indicating which neuroanatomical signs or patterns are most informative[8]. In short, we still lack a precise, reproducible disease fingerprint specifying which alterations occur and where they localize in the brain of patients with DoC. Achieving this could allow to map these alterations onto identifiable neurobiological systems and inform actionable plans for therapeutic intervention.

In establishing a disease fingerprint for DoC, relying on patients with a prolonged DoC (pDoC, ≥28 days post-injury) is particularly advantageous. For instance, neurophysiological readouts are less confounded by sedation/anesthesia, which is common in acute critical care[10]. Additionally, the slower clinical evolution[11] presented by patients with a prolonged DoC facilitates behavioral and neurophysiological assessments under arguably stable conditions, improving brain–behavior inferences. However, pDoC is rare (≈0.2–6.1 per 100,000 in Europe)[8], and specialized expertise and resources for high-quality neurophysiology are unevenly distributed[12], yielding many small studies that often test only one or a few metrics in generally heterogeneous samples with varied etiologies (with few exceptions[13,14]). This landscape hampers replicability and synthesis, complicating the identification of a disease-specific fingerprint, assuming that such a unique fingerprint could indeed be identified, i.e., across patients with different pathophysiology and unique patterns of brain injury.

In this paper, we aim to establish the *type* and the *topography* of brain alterations at the basis of pDoC, by isolating the most consistent, *resting-state* neurophysiological findings, with high translational potential. We conduct quantitative effect-size[15] and coordinate-based[16] meta-analyses across the past two decades of EEG/MEG, MRI, and PET literature, incorporating essential unreported quantitative data, where recoverable. We systematically appraise study demographics, methodological quality, and

evidential strength. We base this multimodal meta-analysis on neurophysiological tools with millisecond temporal resolution, like magnetoencephalography (MEG) and EEG, to answer the question of *which* features of neural activity are globally lost in pDoC. We use neurophysiological tools with millimetric spatial resolution, like MRI and PET, to answer the question of *where* cerebral integrity – i.e., loss of structure, neural and molecular function - is precisely lost in pDoC. We also include an emerging technology, i.e., functional near-infrared spectroscopy (fNIRS), as a promising, highly portable tool for DoC assessment[17]. To bridge circuits to biology, we relate the resulting cross-modal convergence map to independent, multi-level normative datasets, including human molecular-imaging atlases of neurotransmission, thereby exposing specific mechanistic hypotheses and actionable gaps to guide future research and clinical translation.

Results

Studies and population characteristics

Screening - Literature search in MEDLINE, Scopus and EMBASE for neurophysiological studies of patients with pDoC resulted in identification of a total of 7,450 (883 PET/single photon emission computed tomography (SPECT), 2,415 MRI, 72 fNIRS and 4,080 EEG/MEG) potentially eligible studies. After screening abstracts and full-texts, we identified 53 EEG[13,14,18-68], 19 PET[18,38,50,69–84] and 26 MRI[18,50,70,85–107] studies, for a total of n=90 (including 6 multimodal[28,31,44,73,79,82]) resting-state studies assessing predominantly adult patients with pDoC, after awakening from coma (i.e., UWS/VS and MCS), with clinical assessment based on a validated clinical scale (**Figure 1**). We identified no studies using MEG, fNIRS or SPECT fitting our inclusion criteria.

Study and population characteristics – We included 90 studies published between 2003 and 2023, based on data obtained in 32 recruiting centers located in 12 different countries in Asia, Europe and America, including a median of 27 pDoC patients per study (**Figure 2A**). Included studies reported PET, MRI and EEG findings from 1,372 observations in healthy volunteers and 3562 observations in pDoC patients (n=1,817, 51.01% UWS/VS; n=1,718, 48.23% MCS). Detailed demographical and clinical information relative to the specific participants undergoing the neurophysiological assessments of interest was missing in 205 (14.94%) of healthy volunteers observations (286 (8.02%) of pDoC) for sex, 225 (15.98%) of healthy volunteers observations (313 (8.79%) of pDoC) for age, and 499 (14%) and 461 (12.94%) of pDoC patients for etiology and time since injury, respectively. Males were slightly overrepresented in both healthy volunteers (M: n=609, 44.38%; F: n=558, 40.61%) and pDoC patients (M: n=1,995, 56%; F: n=1,281, 35.96%)($\chi^2(2, n=4934)=78.78$, $p<.001$). The estimated average age was 42.74±13.63 (5.8-80) years in the healthy volunteers and 46.01±14.22 (5-90) years in pDoC, with healthy older participants slightly underrepresented ($t(4932)=-7.32$, $p<.001$, Hedges' $g=0.23$). Etiology of the pDoC patients was 1.60 times more likely to be non-traumatic (n=1,884 (52.89%), including 574 (16.12%) of anoxic cases) than traumatic (n=1,179, 33.10%). Estimated time since injury was of 30.93±32.31 (0-423) months, with 26 (29.54%) studies including primarily (>95%) pDoC observations less than 12 months since injury (**Figure 2B**).

Quality of evidence – Among 53 EEG, 19 PET and 26 MRI studies, 64 were cross-sectional case-control studies comparing DoC patients against healthy volunteers. According to a 7-item adapted version of the Newcastle Ottawa Scale (NOS) (**Supplementary Table 1**), the median quality of evidence was 3.5 (IQR: 2.5-4; range: 2-7) (**Table 1**). The lowest scores were obtained for the selection of controls, with 60 (93.8%) studies not including or not providing adequate information on inclusion of *community* controls. Forty-

three (67.2%) studies did not include or did not report details about definition of the controls, and 43 (67.2%) about the representativeness of the cases. While most studies did not explicitly state whether cases and controls were comparable by age (n=51, 79.69%) or sex (n=58, 90.66%), the majority did include comparable cases and controls (n=37, 57.8% for age and n=43, 67.2% for sex). All studies, per inclusion criteria, defined ascertainment of exposure adequately.

A 3-item adapted version of the NOS, excluding items relative to controls, was used to assess the remaining 34 cross-sectional studies, comparing DoC patients between each other with a median quality of evidence of 3 (IQR: 2-3; range: 2-3).

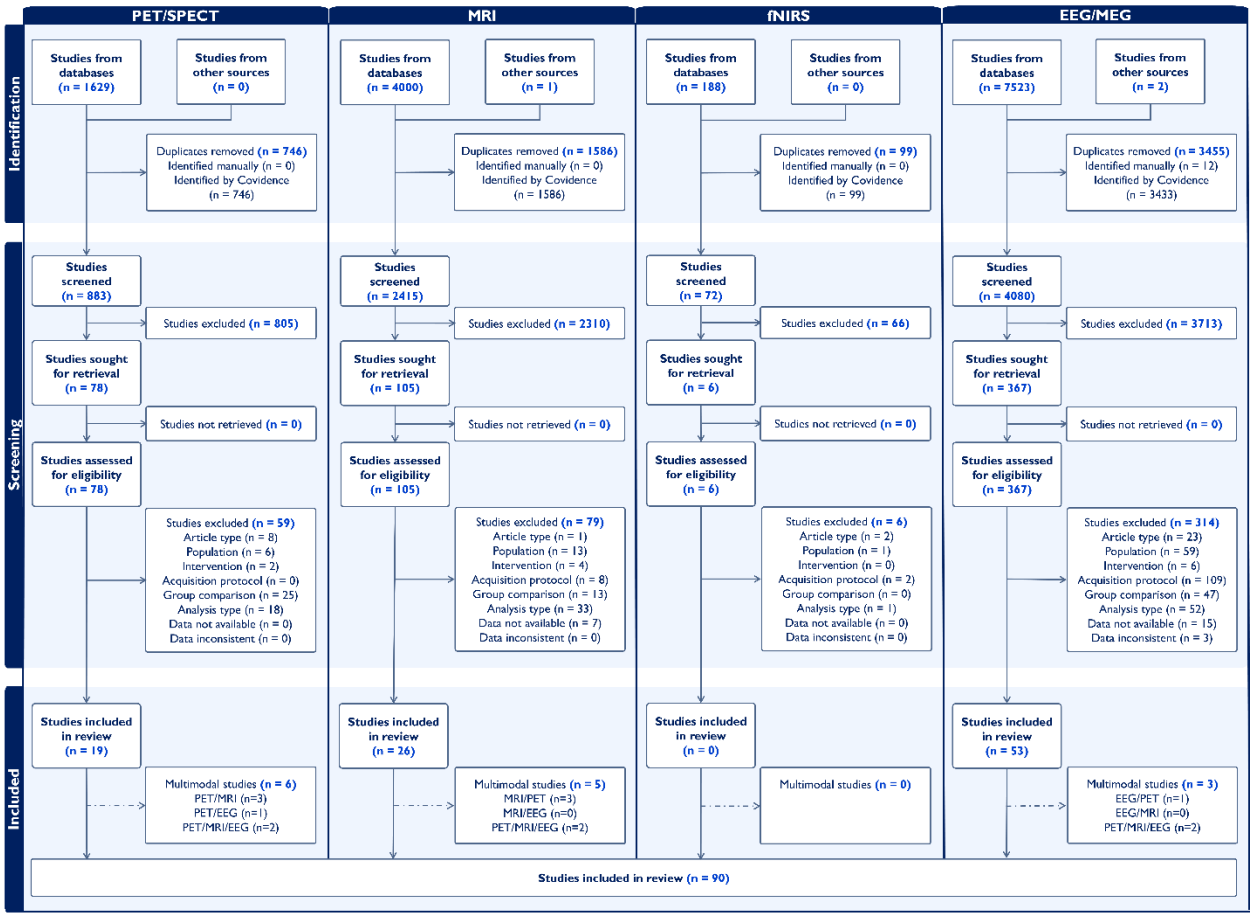

Figure 1. PRISMA (2020) flow diagrams for study selection

[The high resolution figure can be visualized at:
https://drive.google.com/file/d/11Mzd6zR9W8gqSBzsH9QFwbMTNyB3T0mQ/view?usp=sharing*]*

Abbreviations: EEG, electroencephalography; fNIRS, functional near-infrared spectroscopy; MEG, magnetoencephalography; MRI, magnetic resonance imaging; PET, positron emission tomography; SPECT, single-photon emission computed tomography.

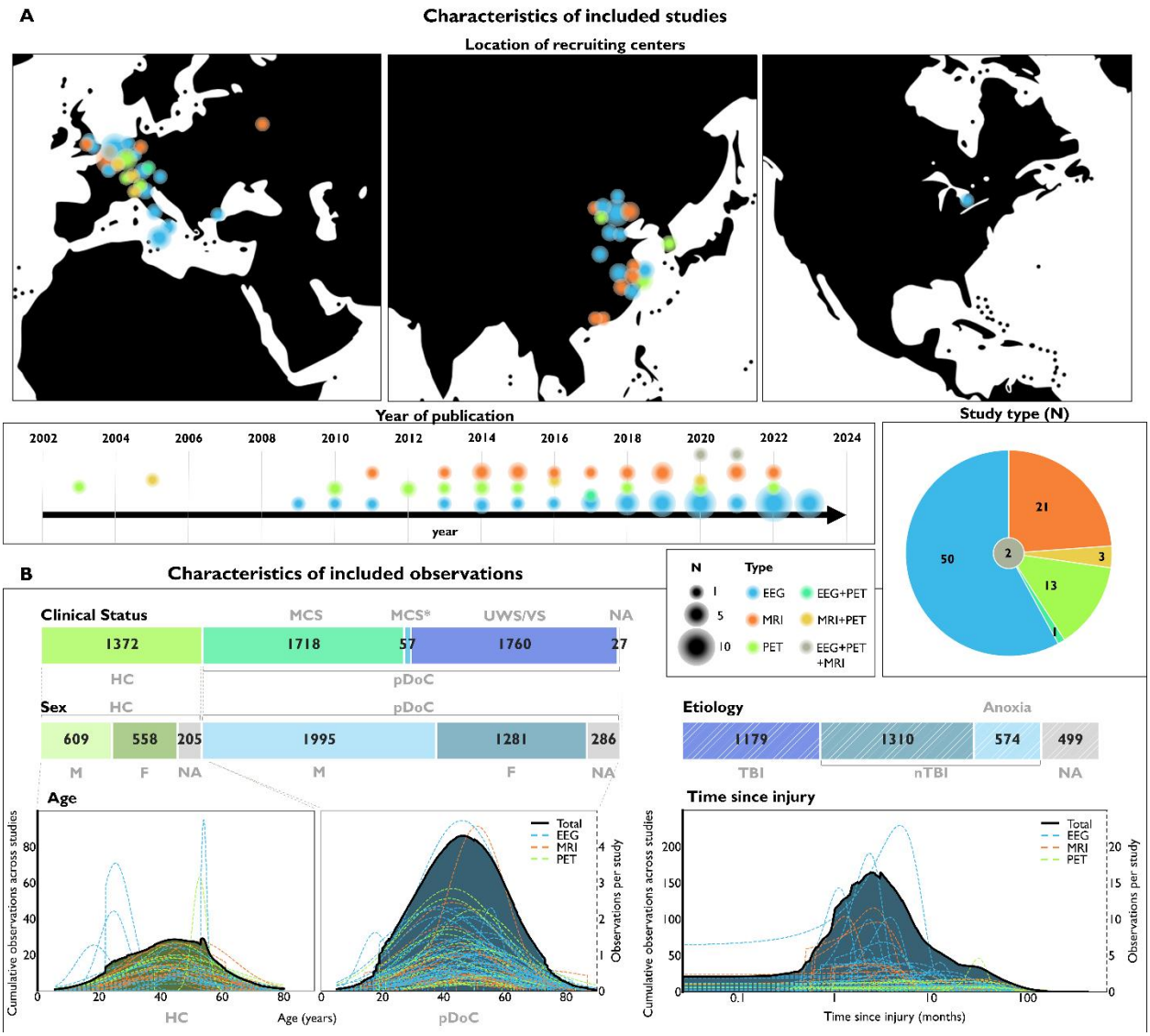

Figure 2. Overview of included studies and observations. (A) *Characteristics of included studies.* Map shows the geographic locations of recruiting centers. Size of bubbles is proportional to the number of studies using data of a given center. Timeline shows the year of publication of included studies. Size of bubbles is proportional to the number of studies published in a given year. Sunburst plot shows the proportion of studies based on the type of neurophysiological tool included in the meta-analysis. **(B)** Characteristics of included observations. Stacked bar charts show distributions of included observations by clinical status, sex and etiology of brain injury, respectively. Probability density function plots show the estimated number of observations with a given age (in years) or time since injury (in months) across all studies (left y axis, continuous line) and per study (right y axis, dotted lines). *[The high resolution figure can be visualized at:* https://drive.google.com/file/d/13Ji-foEkQ2LZXPGhfYglC75yhV0NwAh8/view?usp=sharing*]*

Abbreviations: EEG, electroencephalography; HC, healthy controls; MCS, minimally conscious state; MCS, minimally conscious state star; MRI, magnetic resonance imaging; nTBI, non-traumatic brain injury; pDoC,*

prolonged disorders of consciousness; PET, positron emission tomography; TBI, traumatic brain injury; UWS/VS, unresponsive wakefulness syndrome/vegetative state.

Electrophysiological findings

Random-effects meta-analyses of EEG, MEG and fNIRS findings were performed to evaluate *which* features of neural activity are globally lost in pDoC. Fifty-three EEG, 0 MEG and 0 fNIRS studies investigating neurophysiological changes at the global brain level were eligible for inclusion in the random-effects meta-analyses. These studies investigated 335 distinct global (i.e., whole brain) neurophysiological features overall. Among all studies, 28 included 228 neurophysiological features in pDoC patients and healthy volunteers, and 46 included 315 neurophysiological features in UWS/VS against MCS patients. Out of 335 features, 221 (65.97%) could be grouped into 143 subfamilies of analogous features across different frequency bands (**Supplementary Table 2**). As the recommended threshold for random-effects meta-analysis is of five studies[108], we hereby describe the results of 11 random-effects meta-analyses on subfamilies of analogous features in a total of 11 studies comparing pDoC patients against healthy volunteers and of 38 random-effects meta-analyses in a total of 39 studies comparing UWS/VS against MCS patients. In **Supplementary Tables 3-6**, we report results of the primary and secondary comparisons of interest based on at least five studies.

Differences in pDoC neurophysiology

Study characteristics – The n=11 EEG studies comparing global neurophysiological features in pDoC patients against healthy volunteers and n=39 EEG studies comparing UWS/VS against MCS, relied respectively on three (power spectral density (PSD), connectivity and graph theory) and six (PSD, connectivity, graph theory, microstates, entropy and complexity) families of EEG features over a total of 549 and 1,474 observations. EEG features were obtained with caps of various densities (8-256 electrodes), with data predominantly analyzed at the scalp level (n=9 studies, 81.82% and n=35 studies, 89.74%, respectively). Acquisitions were carried out predominantly with eyes open (n=8, 72.72%) for studies comparing pDoC patients against healthy volunteers, and more variable settings (eyes open n=13, 30%, closed n=5, 12.82%) for studies comparing UWS/VS and MCS. Information on sedation was not reported in n=10, 90.91% and in n=18, 46.15% studies, respectively (**Figure 3A**).

Meta-analyses (pDoC vs. healthy volunteers) – **Figure 3B** shows the standardized mean difference (SMD) and relative confidence interval (CI) for the 11 meta-analyses, based on 5 to 8 studies (**Supplementary Table 3**). Compared to healthy volunteers, pDoC patients showed (i) significantly reduced relative power in alpha (SMD: -2.36, 95% CI [-3.00,-1.73]) and beta (-1.31, [-1.76,-0.86]) bands and significantly increased relative power in the delta band (2.00, [1.60,2.39]); (ii) significantly reduced connectivity in alpha (-1.23, [-1.63,-0.83]) and beta (-0.44, [-0.86,-0.02]) bands and significantly increased connectivity in the delta (2.00, [1.60,2.39]) and theta (0.41, [-0.43,1.24]) bands. All significant effects reported were large, except for connectivity in beta and theta (medium). Results were confirmed in overall n=24 sensitivity analyses (n=0-4 sensitivity analyses per each meta-analysis), i.e., they were robust to choice of specific EEG feature, imputation, clinical subpopulation and outliers[35,63], with the exception of the result of decreased connectivity in the beta band, which did not survive removal of an outlier[35]. Heterogeneity was significant across all meta-analyses, ranging from substantial to considerable (median I^2: 0.74, IQR: 0.71-0.89, range: 0.62-0.93) (**Supplementary Table 3**). Heterogeneity was solved by removal of an outlier[35] in 4 (36.36%) meta-analyses. Publication bias could not be reliably assessed due to the low (N<10) number of studies.

Figure 3. Overview of included EEG studies and converging alterations in global features of neural activity in pDOC. (A) Characteristics of the n=11 and n=39 EEG studies included for the pDoC vs. healthy volunteers and UWS/VS vs. MCS comparisons, respectively. Bar charts show distribution of studies by

number of electrodes used, acquisition setting (i.e., eyes open, closed vs. not controlled for; sitting or lying), use of sedation (i.e., none vs. possible in some patients), and level of data analysis (scalp vs. source). The number of studies available per family of EEG measures, for each band and broadband, is also shown. **(B)** Converging alterations in global features of neural activity are denoted in red for pDoC patients vs. healthy volunteers (left) and UWS/VS patients vs. MCS patients (right), as deemed significant at $p<0.05$ uncorrected for multiple comparisons. Each row shows the pooled standardized mean difference and 95% confidence interval for each of n=49 meta-analyses. The hashtag denotes significant effects that could not be replicated in at least one of the n=78 sensitivity analyses. *[The high resolution figure can be visualized at: https://drive.google.com/file/d/1LJkDhKkZxCbTHUoS7Oupa3cF9XOuH9iN/view?usp=sharing]*

Abbreviations: BB, broadband; DoC, disorders of consciousness; EEG, electroencephalography; HC, healthy controls; MCS, minimally conscious state; NA, not available; NC, not controlled for; *pDoC, prolonged disorders of consciousness;* PSD, power spectral density; SMD, standardized mean difference; *UWS/VS, unresponsive wakefulness syndrome/vegetative state.*

Meta-analyses (UWS/VS vs. MCS) - **Figure 3B** shows the SMD and CI for the 39 meta-analyses, based on 5 to 16 studies (**Supplementary Table 4**). Compared to MCS patients, UWS/VS patients showed (i) significantly reduced relative power in theta (-0.34 [-0.50,-0.18]) and alpha (-0.48 [-0.80,-0.16]) bands and significantly increased relative power in the delta band (0.36 [0.05,0.68]); (ii) significantly reduced connectivity in alpha (-0.59 [-0.87,-0.31]) and beta (-0.48 [-0.92,-0.05]) bands; (iii) significantly reduced standard deviation of the participation coefficient (related to the presence of connectivity hubs) in the theta (-0.49 [-0.77,-0.21]), alpha (-1.06 [-1.82,-0.31]) and beta (-0.68 [-1.19,-0.18]) bands; (iv) significantly reduced broadband entropy (-1.01 [-1.53,-0.48]) and complexity (-0.61, [-1.16,-0.06]). All significant effects reported were medium, except for broadband entropy and standard deviation of the participation coefficient in the alpha band (large). Results were confirmed in overall n=54 sensitivity analyses (n=0-4 sensitivity analyses per each meta-analysis), i.e., they were robust to the choice of EEG sub-band, specific EEG feature, imputation, clinical subpopulation and outliers[28,33,35,51], with the exception of the result of decreased connectivity in the beta band, which did not survive after choice of a different beta sub-band; further, non-significant results for theta connectivity and absolute power became significant after excluding input based on imputation and one outlier, respectively. Heterogeneity was significant across 19 (48.72%) out of all meta-analyses, ranging from not important to substantial (median I^2: 0.39, IQR: 0.00-0.70, range: 0.00-0.84) (**Supplementary Table 4**). Heterogeneity was solved by removal of an outlier, among[28,33,35,51], in 9 out of 19 (47.37%) heterogeneous meta-analyses. Publication bias could be assessed for ten EEG metrics; no asymmetry was observed in the funnel plots of either metric, confirmed by Pustejovsky and Rodgers version of the Egger's test[109] indicating no significant publication bias.

Neuroimaging findings

Random-effects coordinate-based meta-analysis was performed to evaluate *where* structural, functional and molecular cerebral integrity is altered in pDoC. Fourteen PET, 21 MRI and five PET/MRI voxel-wise, whole-brain studies were eligible for inclusion in the coordinate-based meta-analysis. All studies investigated structural, functional and molecular differences in the gray matter, with the exception of one white matter study[110]. Among studies in the gray matter, 39 compared pDoC patients against healthy volunteers, with 40 experiments evaluating decreased and 17 experiments evaluating relative preservation of cerebral integrity in pDoC, and 10 evaluating decreased cerebral integrity in UWS/VS against MCS patients. As the recommended threshold for coordinate-based meta-analysis is of 20

experiments[111], we here describe the results of coordinate-based meta-analysis of decreased cerebral integrity comparing pDoC patients against healthy volunteers, and evaluate the contributions of UWS/VS and MCS groups per cluster when available. We report results of each primary and secondary comparison of interest (including exploratory meta-analyses based on 10-19 experiments) in **Supplementary Tables 7-11** and in the Zenodo database.

Decreased cerebral integrity in pDoC

Study characteristics - Of the 39 PET and MRI studies investigating decreased cerebral integrity in pDoC patients, the great majority reported findings based on [^{18}F]FDG-PET imaging of glucose metabolism (N=19, 48.72%) and/or functional MRI imaging of blood-oxygen level dependent (BOLD) signal (n=21, 53.85%). Acquisitions were carried out with variable resting condition settings (eyes open n=5, 12.83%; closed n=9, 23.08%), with the majority (25, 64.1%) of studies not reporting or not controlling for the latter. Information on sedation (n=12, 30.77% no sedation; n=4, 10.26% possible) was not reported in n=23, 58.97% of studies (**Figure 4A**).

Coordinates characteristics - The majority (n=580, 72.23%) of coordinates were reported by fMRI studies, followed by PET (n=172, 21.42%) and sMRI (n=51, 6.35%) studies. All sMRI coordinates were derived from comparisons of measures of voxel-based morphometry; the majority of PET coordinates (n=166, 96.51%) from measures of relative glucose metabolism, with scaling to the global mean in 86.75% (n=144) of reported coordinates; the majority of fMRI coordinates from comparisons of various functional connectivity measures (n=520, 89.66%) or intensity of spontaneous fluctuations (n=46, 7.93%) (**Figure 4B; Supplementary Table 12**).

Coordinate-based meta-analysis in pDoC - The coordinate-based meta-analysis (based on 39 studies, 40 experiments and 1,156 subjects) indicated converging decreases in eight clusters, with findings in each cluster supported on median by n=12 independent experiments (range: 10-30), with a median average non-linear contribution per experiment of 4.46% (range: 0.09-21.30%) indicating robust meta-analytical findings. We found converging decreases in cerebral integrity in the subcortical regions of the thalamus, mainly in the mediodorsal nucleus (89.29% of this nucleus [55.28% of assigned voxels in the thalamic cluster]), central lateral nucleus (37.62% [15.47%]), centre median nucleus (32.77% [4.7%]) and ventral later posterior nucleus (21.8% [15%]), and the caudate nucleus, almost exclusively in its executive subdivision (13.13% [98.7%]). At cortical level, decreases in cerebral integrity converged almost exclusively within the boundaries of the default mode network (DMN) (7.59% [99.6%]), and specifically on the precuneus (mainly area 7m (39.62% [29.53%])), posterior cingulate gyrus (primarily area d23ab (63.98% [33.66%]), plus v23ab (31.25% [10.8%])) and angular gyri (primarily area PGi (27.5% [62.85%]), plus PGs (11.66% [20.82%])), bilaterally. Significant clusters were reported at the level of the medial prefrontal cortex (primarily area 9m (2.88% [68.73%])) and medial orbitofrontal gyrus (primarily area 10v (2.63% [48.25%])). Results were deemed significant at a cluster-level $p<0.05$ FWE-corrected statistical threshold and a voxel-level uncorrected $p<0.001$ cluster-forming threshold (**Figure 4C; Supplementary Table 7**).

UWS/VS vs. MCS contribution analysis – Leveraging available information on specific clinical sub-populations of pDoC, we evaluated the non-linear contribution of UWS/VS and MCS to the meta-analytical results in pDoC: (i) MCS contributed predominantly to subcortical alterations (median contribution of 41.86% by MCS, 21.33% by UWS/VS); (ii) UWS/VS contributed predominantly to cortical alterations

(UWS/VS: 50.64%, MCS: 17.41%); (iii) UWS/VS and MCS jointly contributed to alterations in the thalamus (UWS/VS: 38.92%, MCS: 41.86%) and precuneus/posterior cingulate (UWS/VS: 43.57%, MCS: 30.21%) (**Figure 4C**). Results of the exploratory meta-analyses in UWS/VS and MCS are reported in **Supplementary Results and Tables 10-11**.

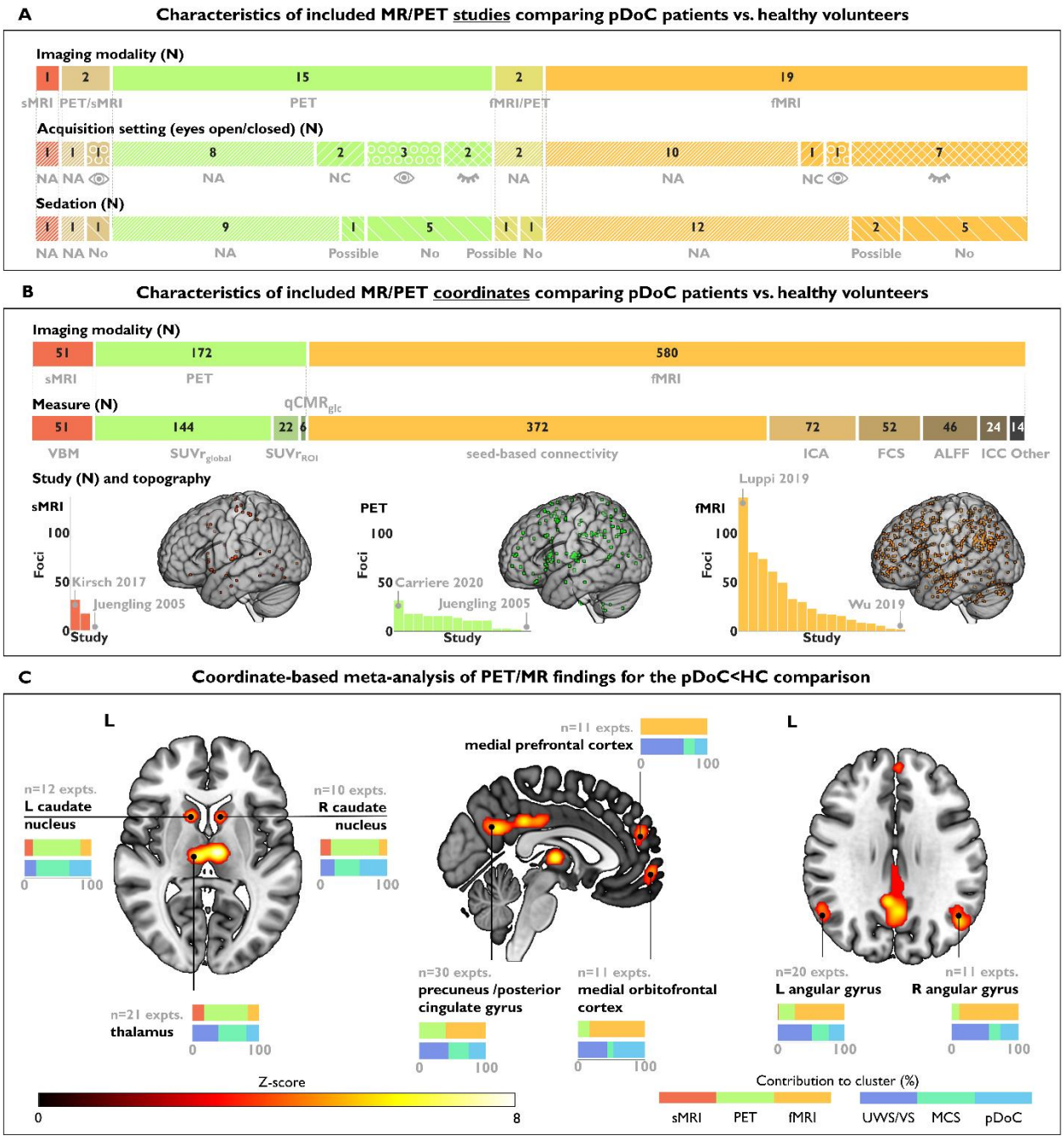

Figure 4. Overview of included MRI/PET studies and converging areas of decreased cerebral integrity in pDOC. (A) Characteristics of the n=39 included MRI/PET studies. Bar charts show distribution of studies by imaging modality, acquisition setting (i.e., eyes open, closed vs. not controlled for) and use of sedation (i.e., none vs. possible in some patients). **(B)** Characteristics of the n=803 known locations of decreased cerebral integrity. Bar charts show distribution of coordinates by imaging modality, measure of interest

and study. Brain renders show spatial localization of coordinates in Montreal Neurological Institute (MNI) space. (**C**) Clusters of significant spatial convergence of the n=803 known locations of decreased cerebral integrity. Clusters surviving a cluster-level p<0.05 FWE-corrected statistical threshold and a voxel-level uncorrected p<0.001 cluster-forming threshold are shown. The number next to each cluster's label indicates the amount of independent experiments directly contributing to that cluster. Bar charts show the average non-linear contribution of different features, i.e., imaging modality (sMRI, PET, fMRI) and clinical group (UWS/VS, MCS or pDoC) to each cluster. The pDoC label refers to experiments where UWS/VS and MCS are analyzed jointly, so that the contribution of each clinical group cannot be estimated. Brain renders were created using MRIcroGL (https://github.com/rordenlab/MRIcroGL). *[The high resolution figure can be visualized at:* https://drive.google.com/file/d/15cu0HEI3ikCLxx8QGL5vVLzWOdU9DbcM/view?usp=sharing*]*

*Abbreviations: ALFF, amplitude of low frequency fluctuations; FCS, functional connectivity strength; f*MRI, functional magnetic resonance imaging; ICA, independent component analysis; ICC, intrinsic connectivity contrast; MCS, minimally conscious state; *NA, not available; NC, not controlled for;* pDoC, prolonged disorders of consciousness; PET, positron emission tomography; *$qCMR_{glc}$, quantitative measure of the cerebral metabolic rate of glucose; sMRI, structural magnetic resonance imaging; SUV_{global}, standardized uptake value scaled to the global mean; SUV_{ROI}, standardized uptake value scaled to a region of interest;* UWS/VS, unresponsive wakefulness syndrome/vegetative state; *VBM, voxel-based morphometry.*

MRI vs. PET contribution analysis - The contribution analysis showed that PET and sMRI predominantly accounted for subcortical clusters, whereas fMRI mainly contributed to cortical clusters, except in the precuneus/posterior cingulate region, where both PET and fMRI contributed considerably (Figure 4C; **Supplementary Results**). Results of the exploratory meta-analyses in each imaging modality, are reported in **Supplementary Tables 13-14**.

Spatial correlation with an independent panel of multi-level neurobiological data

To characterize the biological mechanisms underlying decreased cerebral integrity in pDoC patients, we contrasted the unthresholded meta-analytical Z-score map derived from the 39 studies above (**Figure 5A**), representing the likelihood of decreased cerebral integrity associated to pDoC to occur in each voxel, against the spatial distribution of 65 neurobiological features of the human brain, as obtained from an independent sample of n=5,215 individuals. Significance of spatial correlations was set at p<0.05 after Bonferroni correction for multiple comparisons within each map type, as robustly estimated based on three methods for random null-map generation, iterations adaptively adjusted. Spatial correlation with *cortical* brain maps showed that decreased cerebral integrity in pDoC followed (i) a unimodal-transmodal functional and (ii) an evolutionary hierarchy, with higher-order associative areas and cortical areas that expanded the most in the evolution from macaque to human, most likely to be affected in pDoC (**Figure 5B**). Spatial correlation with *whole* brain maps showed that loss of cerebral integrity in pDoC was most likely to occur in areas typically sustaining higher neural activity (as supported by higher perfusion, glucose metabolism and synaptic density) (**Figure 5C**). Comparison against neurotransmission systems showed that the likelihood of brain alterations in pDoC was significantly and reliably associated with specific post-synaptic elements within the non-monoaminergic systems, namely expression of excitatory metabotropic glutamatergic 5 (mGLU5) receptors, inhibitory metabotropic mu-opioid and cannabinoid 1 (CB1) receptors and inhibitory ionotropic gamma-aminobutyric acid A (GABA-A) receptors. Among monoaminergic transmitters, we found a reliable association with the pre-synaptic noradrenaline transporter.

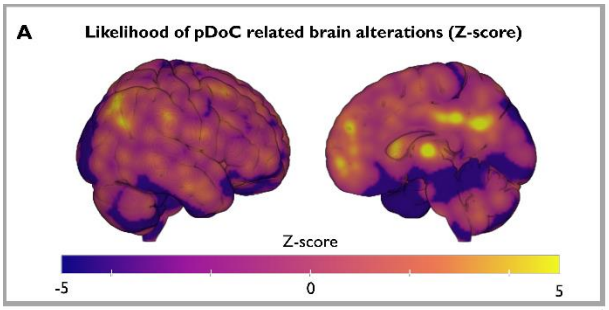
A
Likelihood of pDoC related brain alterations (Z-score)
Z-score
-5
0
5

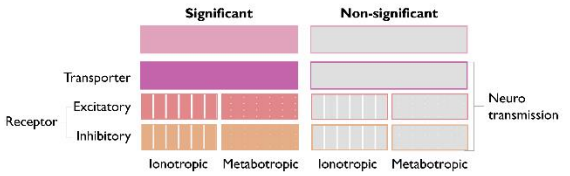
Significant
Non-significant
Transporter
Receptor
Excitatory
Inhibitory
Neuro transmission
Ionotropic
Metabotropic
Ionotropic
Metabotropic

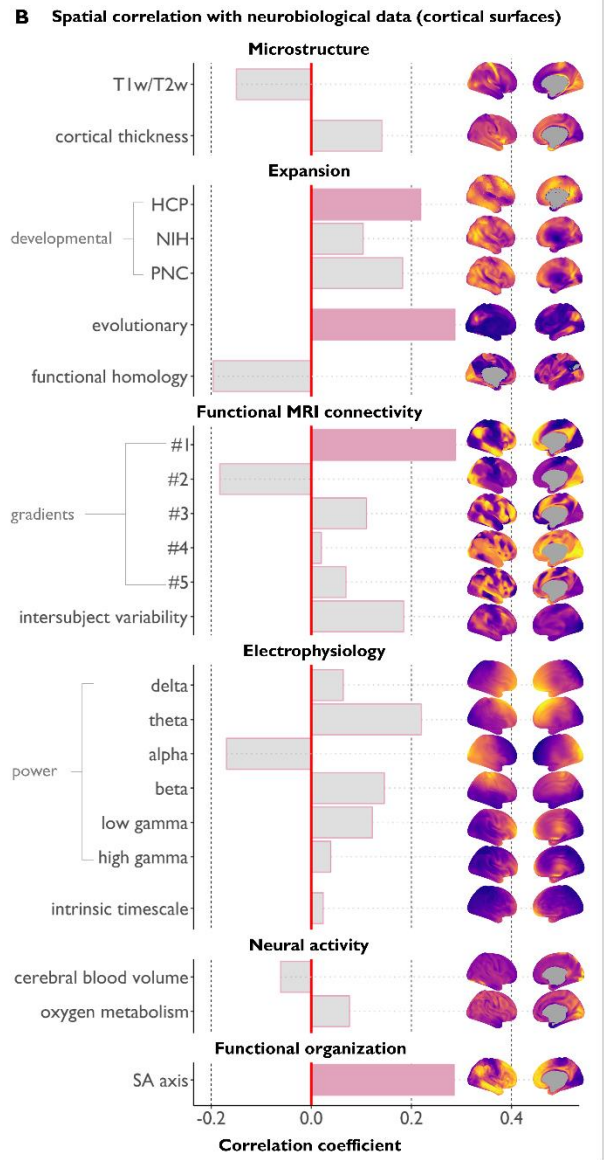
B
Spatial correlation with neurobiological data (cortical surfaces)
Microstructure
T1w/T2w
cortical thickness
Expansion
developmental
HCP
NIH
PNC
evolutionary
functional homology
Functional MRI connectivity
gradients
#1
#2
#3
#4
#5
intersubject variability
Electrophysiology
power
delta
theta
alpha
beta
low gamma
high gamma
intrinsic timescale
Neural activity
cerebral blood volume
oxygen metabolism
Functional organization
SA axis
-0.2
0.0
0.2
0.4
Correlation coefficient

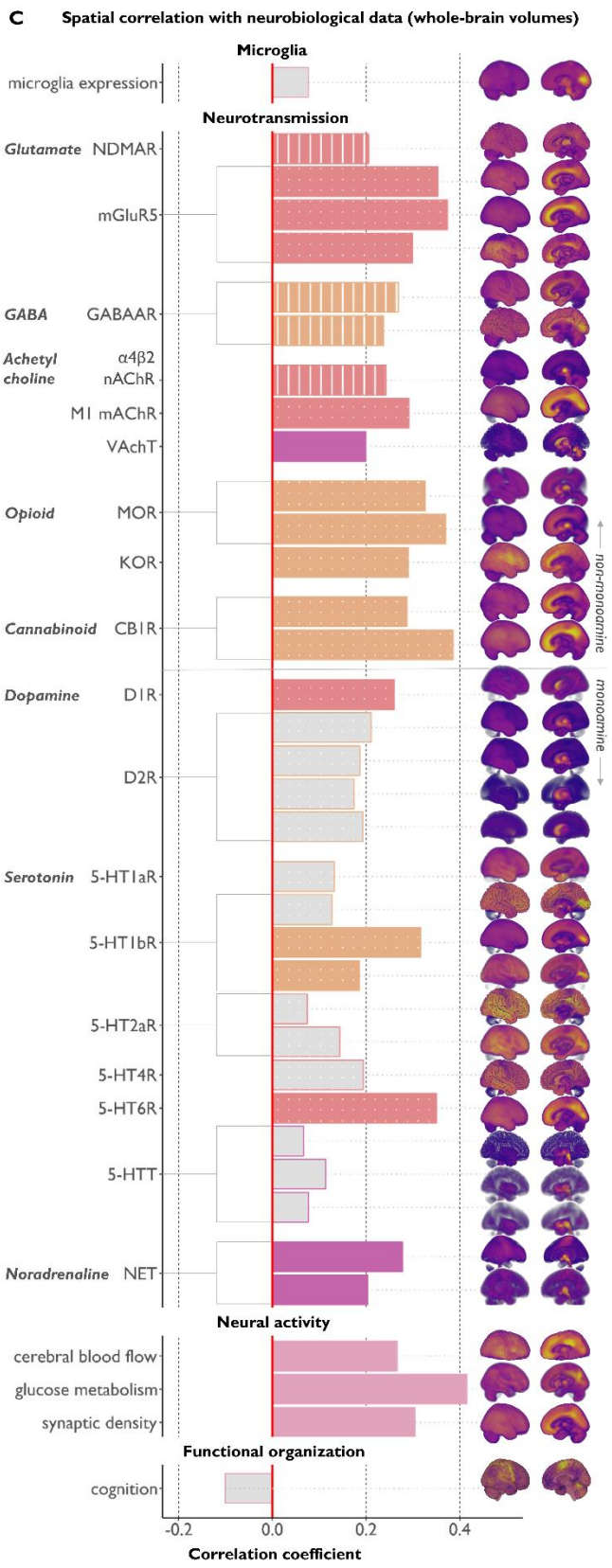
C
Spatial correlation with neurobiological data (whole-brain volumes)
Microglia
microglia expression
Neurotransmission
Glutamate
NDMAR
mGluR5
GABA
GABAAR
Achetyl choline
α4β2 nAChR
M1 mAChR
VAchT
Opioid
MOR
KOR
Cannabinoid
CB1R
Dopamine
D1R
D2R
Serotonin
5-HT1aR
5-HT1bR
5-HT2aR
5-HT4R
5-HT6R
5-HTT
Noradrenaline
NET
non-monoamine
monoamine
Neural activity
cerebral blood flow
glucose metabolism
synaptic density
Functional organization
cognition
-0.2
0.0
0.2
0.4
Correlation coefficient

Figure 5. Spatial correlation between likelihood of decreased cerebral integrity in pDoC and spatial distribution of neurobiological brain features. (**A**) Brain render of the meta-analytical map of decreased cerebral integrity in pDoC (unthresholded). Positive Z-score values indicate above-chance likelihood of finding decreased cerebral integrity for a given voxel. (**B**) Bar charts denote the magnitude of Pearson's correlation coefficient between likelihood of pDoC-related brain alterations and a wide range of neurobiological, i.e., microstructural, functional, electrophysiological and organizational cortical features. Colored vs. gray bars denote significant vs. non-significant correlations at p<0.05 Bonferroni-corrected for multiple comparisons. Level of spatial expression of each cortical feature is shown in surface renders created with *Matplotlib* (https://matplotlib.org/stable/). (**C**) Bar charts denote the magnitude of Pearson's correlation coefficient between likelihood of pDoC-related brain alterations and a wide range of neurobiological molecular brain features. Colored vs. gray bars denote significant vs. non-significant correlations at p<0.05 Bonferroni-corrected for multiple comparisons. Bars for the neurotransmission panel are further color-coded for transporters, excitatory/inhibitory and ionotropic/metabotropic receptors. Level of spatial expression of each brain feature is shown in brain renders created with *MRIcroGL* (https://github.com/rordenlab/MRIcroGL). *[The high resolution figure can be visualized at: https://drive.google.com/file/d/1NHefjZKxthdbqjOIMImcPhgiqMyKX_Pl/view?usp=sharing]*

Abbreviations: *α4β2 nAChR, alpha4beta2 nicotinic acetylcholine receptor; 5-HT_R, serotonin receptor; 5-HTT, serotonin transporter; CB1R, cannabinoid receptor type 1; D1R, dopamine receptor D1; D2R, dopamine receptor D2; DoC, Disorders of Consciousness; GABAAR, gamma-aminobutyric acid a receptor; HCP, Human Connectome Project; KOR, kappa-opioid receptor; M1 mAChR, muscarinic acetylcholine receptor M1; mGluR5, metabotropic glutamate receptor 5; MOR, mu-opioid receptor; NET, norepinephrine transporter; NMDAR, N-methyl-D-aspartate receptor; NIH, National Institutes of Health; pDoC, prolonged disorders of consciousness; PNC, Philadelphia Neurodevelopmental Cohort; SA axis, somatosensory to associative axis; T1w/T2w, T1-weighted / T2-weighted ratio; VAChT, vesicular acetylcholine transporter.*

Discussion

In this multimodal meta-analysis, we provide the most comprehensive quantitative synthesis of resting-state neurophysiological alterations in patients with pDoC to date. By establishing the *type* of physiological alterations and the *topography* of structural, functional and molecular damage in the pDoC population, we isolate the most consistent findings, providing markers with high translational potential. Integrating reported and recovered (previously unreported) results from a total of 90 studies and 3,535 EEG, PET and MRI observations acquired with heterogeneous protocols and hardware, our main findings in pDoC were three-fold: (i) a robust global shift in neural activity toward stronger delta and weaker alpha power and connectivity; (ii) anatomically precise, cross-modal loss of structure, function and metabolism centered on subcortical "integration zones" of the mediodorsal thalamus and the executive subdivision of the caudate nucleus, together with specific cortical hubs of the DMN; and (iii) a preferential association of these alterations with non-monoaminergic neurotransmission - excitatory glutamatergic and inhibitory GABAergic systems - and, to our knowledge for the first time in DoC, modulatory opioid and cannabinoid systems. We also found that broadband entropy and alpha-standard deviation of the participation coefficient best discriminate among unresponsive and minimally conscious patients. Below, we discuss in further detail each of these findings.

First, we found that patients with a pDoC show a consistent slowing of the global power spectrum, with decreased oscillatory power and connectivity in the *alpha* band, and increased oscillatory power and

connectivity in the *delta* band. The former might derive from the amplification of tonic firing of the thalamus by cortical neurons receiving intact thalamocortical afferents[112], whereby the latter is observed in the cortex under pathological deafferentation[113] and pharmacological or physiological[114] decoupling of the thalamus and subsequent disfacilitation of the cortex. This electrophysiological profile aligns well with our robust observation (in n=24 experiments) of structural, functional and molecular loss of integrity in the thalamus of pDoC patients. Interestingly, while duration of alpha oscillatory events depends on GABAergic receptors, the frequency of the oscillations seems to be modulated by activation of metabotropic glutamatergic signalling[115]. These are receptors we find highly expressed within regions showing decreased cerebral integrity in pDoC (**Figure 5**). Notably, following reduced glutamatergic input[116], *theta* oscillations can emerge as a slowing of alpha oscillations, a mechanism that might explain the lack of a significant decrease in theta power observed in pDoC patients (**Figure 3**). The global preservation of theta power in pDoC may result from heterogeneous and potentially widespread regions with preserved function, as cortical regions functioning in isolation tend to resonate around 7 Hz[117]. The observed increase in theta connectivity in pDoC is also consistent with this hypothesis, as theta connectivity in the healthy brain is associated with DMN function specifically, and thus spatially restricted[118]. We also observed a robust *beta* band decrease, which may reflect a cortical generator alone[119] and/or extrinsic synaptic drive from basal ganglia (including striatal medium spiny neurons)[120] or thalamus[121]; this dovetails with our evidence for loss of integrity in cortex and subcortex (thalamus and caudate; **Figure 4**). Subgroup analyses showed that UWS/VS patients exhibit higher *delta* power and lower *alpha* power/connectivity than MCS patients. By contrast, *theta* power (but not connectivity) was higher in MCS than UWS/VS, which we interpret as better capacity for local theta generation in MCS[7] despite the absence of normal DMN theta dynamics[118]. This aligns with our exploratory anatomical findings of a more spatially restricted loss of DMN integrity in MCS relative to the broader injury seen in UWS/VS. Together, these results support complementary global (thalamocortical) and local (cortical) mechanisms shaping rhythm-specific alterations in pDoC.

Second, we identified anatomically specific decreases in cerebral integrity that partly revise prevailing narratives[71,122]. Cortically, we confirm consistent DMN involvement - precuneus (area 7m), posterior cingulate (d23ab), inferior parietal lobule (PGi), and portions of medial prefrontal cortex (areas 9m/10v) - but, strikingly, we find no cross-study-consistent loss outside the DMN. This challenges the traditional framing of pDoC as a conjoint disorder of "internal" (DMN) and "external" (central executive/frontoparietal) awareness networks[71,122]. Instead this is in accordance with a modern view of the DMN as an integrative system supporting *both* internally directed and stimulus-related cognition by sustaining an ongoing internal narrative or "frames of thought"[123–125] necessary to construct and maintain an experience of subjective continuity[126]. Furthermore, the DMN subregions we identified map preferentially onto activation networks representing the conceptual/narrative self[127,128] rather than the core/bodily self, for which we find no consistent alteration (anterodorsal precuneus[129], middle cingulate[127]), nor in pDoC, nor in UWS/VS alone. Subcortically, we confirm thalamic involvement, predominantly in the mediodorsal nucleus (≈90% of its volume) and partially in the intralaminar nuclei (≈20-40% of their volumes)(see **Supplementary Discussion**). The mediodorsal nucleus, a calbindin-rich matrix nucleus of higher-order thalamus, exerts a broad excitatory influence not only on medial prefrontal cortex[130] (including frontomedial areas like BA 32 and 9m[131]) but also on posterior cingulate[132] and angular gyrus[133], which are both key DMN nodes (**Figure 4**). Together with tract-tracing studies reporting selective connections of the mediodorsal thalamus with the deep layers of areas 23 of the posterior cingulate cortex[132], this may suggest the presence of mediodorsal nucleus‑DMN coupling. In parallel, we show

consistent caudate involvement specific to its executive subdivision, which projects to dorsolateral and medial frontal cortex[134]. Recent precision connectivity mapping[135–137] places both dorsal thalamus and executive caudate within a subcortical "cognitive integration zone" that regulates DMN coupling to other large-scale networks[2], a process known to be disrupted in pDoC[1]. Collectively, our findings demonstrate that pDoC alterations localize to DMN hubs and to subcortical integration zones at the interface between DMN‑executive/salience/ventral-attention[2] networks, allowing to better specify existing pathophysiological models of DoC. Integrating the study of DoC with that of other global states of consciousness where subjective reporting is possible will allow to understand the functional significance of these findings for consciousness versus responsiveness, disentangling the contribution of DMN itself and on the other hand of the interface between DMN and other large-scale networks to either or both.

Third, we found that the topography of decreased *cortical* integrity aligns to uni-to-transmodal and evolutionary expansion axes. The association of transmodal, evolutionary expanded areas to pathologically reduced consciousness/responsiveness seems to be in keeping with the tethering hypothesis. This posits cortical expansion as a mechanism with which transmodal brain areas can evolve to support complex cognitive tasks, by "untethering" from direct roles in input and output systems[138,139]. We also found that the topography of decreased *cerebral* integrity consistently aligns with the expression of several neurotransmission features. This, mostly involved receptors from the non-monoaminergic class that are strongly expressed along cortical midline and subcortical structures, i.e., brain regions with high neural activity, as indexed by high blood perfusion, glucose metabolism and synaptic density (**Figure 5C**). In more detail, our neurotransmission findings pertain three main domains: (1) arousal, (2) large-scale neural communication and (3) fine-tuning of excitatory-inhibitory integration. First, among monoamines, we observed selective, positive associations with the presynaptic noradrenaline transporter (NET), consistent with noradrenergic roles in arousal[140], affecting the cortical signal-to-noise ratio through gain control[141], attentional gating[142], responsiveness to salient stimuli[143], and recent rodent data showing that tonic firing of the locus coeruleus modulates frontal nodes of the DMN[144]. Furthermore, we found robust, positive associations with postsynaptic mGluR5 and GABA-A receptor maps, supporting an excitatory–inhibitory (E/I) imbalance[145] that would steepen the EEG aperiodic slope[146], favoring lower-frequency activity (**Figure 3**). We also identified replicable, positive associations with μ-opioid and CB1 receptor distributions. To our knowledge, this is the first proposal of a direct link between DoC-related loss of brain integrity and opioid/cannabinoid systems (notwithstanding their putative roles in some anesthetic states[147]). Both μ-opioid and CB1 receptors interact with glutamatergic and GABAergic signaling to fine-tune E/I integration, providing a plausible substrate for large-scale rhythm reorganization[148,149]. In detail, mu-opioid receptors inhibit the pre-synaptic release or post-synaptic effects of glutamate and GABA, resulting in sharp changes in neuronal excitability[65,66]. Cannabinoid1 receptors inhibit release of glutamate, GABA and other transmitters[67], and form complexes with mGLU5 receptors to modulate plasticity[68]. Last, both mu-opioid and cannabinoid1 receptors co-localize post-synaptically[64] suggesting an interactive effect on glutamate and GABA. Altogether, these convergences motivate future receptor-informed interventions: mGluR5 modulators (e.g., mavoglurant, a drug close to phase III testing for treating addiction[150]) and agents enhancing cortical gain via noradrenaline reuptake inhibition (e.g., atomoxetine, used to treat ADHD[151]). Such approaches might, in principle, target distributed circuit dysfunction, potentially eliciting broader effects than traditional, focal neurostimulation strategies. Interpretational constraints apply: normative maps are correlational and partly collinear (e.g., transmodal gradient, evolutionary expansion, DMN hubness), so associations should not be taken as causal. Nevertheless, leveraging unthresholded convergence maps, family-wise correction within map types,

replication across different estimation methods for spatial nulls, and an independent population atlas, mitigate circularity and thresholding artefacts. Moving beyond correlative approaches based on normative maps of neurotransmission, ad-hoc prospective PET studies targeting these systems in pDoC will be indispensable to adjudicate causality and guide mechanism-based clinical trials.

Finally, while the quality of the studies included in the current systematic review and meta-analysis was generally acceptable, we could identify some pressing issues with the overall literature in the field. First of all, most studies (in particular EEG ones) do not report statistics in a way that make them usable and re-usable by the scientific community, so that efforts at quantitatively summarizing or simply comparing existing findings require a disproportionate amount of resources, with a tangible risk that a huge (EEG: 92.45%; PET/MRI: 42.55%) portion of the literature will remain unrepresented in further meta-analytical endeavors. Together with standardizing data collection via Common Data Elements[152], authors should ensure to report as a minimum standard mean and standard deviation for EEG findings and peak coordinates for significant PET/MRI findings. Crucially, sharing complete, unthresholded voxel- or vertex-wise statistical maps - also for non-significant contrasts - would markedly enhance reproducibility and enable image-based meta-analyses, increasing power and mitigating publication bias[111]. Second, most studies do not report or do not control for essential factors related to study design (i.e., comparability of healthy controls) and data acquisition (i.e., eye opening and presence of sedation). This risks systematic bias or confounding the results of electrophysiological[153,154], functional[95,155] and, to some extent, molecular markers of neural activity[155]. This information should also be systematically reported by future studies. Third, the literature on electrophysiological measures remains largely focused on proposing novel measures, with sometimes huge effect size reported (once) and very little efforts at replication. Very few studies test a large panel of measures in a systematic way. For this reason, almost half of the (potentially promising) measures reported in the literature remains technically inaccessible to meta-analytical endeavors. Among the 38 classes of electrophysiological features that we could test, we identified only two features, i.e., the standard deviation of the participation coefficient in the alpha band and entropy in the broadband, that presented with large standardized mean differences between UWS/VS and MCS. Fourth, the literature on neuroimaging measures remains largely focused on functional MRI, with less studies investigating molecular measures of glucose metabolism with PET and structural properties with sMRI. No study (fitting our inclusion criteria) could be identified for any of the dozens of molecular markers of neurotransmission, neuropathology and neuroinflammation that are currently available with PET imaging, highlighting a huge gap in current knowledge.

Further strengths and limitations merit note. First, while systematic reviews and meta-analyses on neurophysiological findings in pDoC are available[8,156–159], this work represents the largest effort, including 17-83 more studies than previous endeavors. This expansion was made possible through an extensive and proactive process of outreach and retrieval of unpublished quantitative statistics, allowing us to incorporate data that were previously inaccessible for meta-analytic integration. Still, the literature fitting our inclusion criteria remains predominantly composed of studies from European and Asian centers (Fig. 1), and may therefore lack full geographical representativeness and diversity, underscoring the need for broader inclusion of cohorts from underrepresented regions in future collaborative initiatives. Second, among available coordinate-based meta-analyses[156,160], this represents the first one to comply with the current gold standard for best practices in the field[111]. Unfortunately, the number of available studies does not make it possible to analyze the effects of specific variables of interest (e.g, etiology, presence of covert awareness, time since injury) on current findings, a task for future meta-analyses relying on a larger pool

of studies (provided future studies will test and report such information). In this regard, interpretation of findings in UWS/VS and MCS subgroups, specifically, should be cautious, as results might be confounded by different etiologies, as traumatic etiology is more common in MCS (49.82%) compared to UWS/VS (23.82%) patients; it is possible that a proportion of UWS/VS patients might also be covertly conscious, as only 8.88% of included studies employed information complementary to standardized behavioral assessment, e.g., neurophysiological results, for patient stratification and 0% used active paradigms for covert consciousness. Last, this meta-analysis relies on neurophysiological quantitative results in pDoC, meaning that neurophysiological alterations associated with early negative outcomes and/or non-analyzable neurophysiological data (e.g. due to poor data quality) were not represented in the selected literature and hence in this work.

In summary, this large multimodal meta-analysis delineates a robust disease fingerprint for pDoC. Across hundreds of existing electrophysiological features, we identify 15 replicable global-activity markers which are reliably altered in pDoC. These markers are robust to variability in systems, acquisition, and analysis, thus supporting their relevance for broad clinical translation. We refine the neurobiology of pDoC to a specific subcortical–cortical circuit-mediodorsal thalamus and executive caudate coupled to DMN hubs - with unprecedented anatomical precision, and we map this circuit onto a plausible molecular architecture spanning noradrenergic, glutamatergic, GABAergic, opioid and cannabinoid systems. Building on this finding, it will be essential to invest in *in silico* computational simulations of brain dynamics using detailed biophysical models to test whether -and how- alterations in the identified neurochemical systems could mechanistically lead to the patterns of altered functional connectivity and spectral activity observed in patients (phase 0 clinical trials). Complementarily, pharmacological probe studies with PET imaging could provide rapid experimental validation by assessing target engagement through single-dose interventions and quantifying their acute effects on brain activity and connectivity. These results pave the way to receptor-informed, circuit-targeted therapeutic strategies, and they underscore the need for shared acquisition/analysis/reporting standards in this rapidly expanding field.

Methods

We conducted a systematic review and meta-analysis in accordance with the Preferred Reporting Items for Systematic Review and Meta-Analysis (PRISMA) guideline[161]. The full protocol, including search strategy using controlled vocabulary and keyword terms, is available in the International prospective register of systematic reviews (PROSPERO) with reference CRD42022327151. The patient, intervention, comparator, outcome (PICO) approach is reported in **Supplementary Table 15**.

Article Selection

We included original peer-reviewed studies, including journal articles and conference papers, published in any language starting 1st January 2000, to focus on studies based on neurophysiological tools and a clinical taxonomy in line to the current standard (i.e., after the proposal of diagnostic criteria for both UWS/VS[162] and MCS[163]). To avoid excluding a large portion of the literature[12], we included studies on DoC patients of any etiology with a diagnosis of UWS/VS or MCS based on a validated assessment scale[164], where more than 50% of the participants were i) adults (≥16 years old) and ii) in a pDoC (≥28 days post-injury). We included studies of neurophysiological assessments under resting state, task-free conditions, based on EEG, MEG, fNIRS, [18F]FDG-, [15O]H2O- or other tracer-PET or -SPECT and structural, perfusion

or functional MRI. We included studies comparing patients with pDOC, UWS/VS or MCS against healthy volunteers and against each other. PET, SPECT and MRI studies were included if they ran voxel-based comparisons in the whole-brain gray or white matter, without applying partial volume correction. EEG, MEG and fNIRS studies were included if they ran comparison of global features of neural activity, obtained from electrodes placed across the entire scalp.

Information sources and search strategy

Studies were searched primarily based on bibliographical databases. Other sources complemented this approach, namely (i) expert recommendations and (ii) search in bibliography of previously published literature reviews and meta-analyses. The databases MEDLINE via Ovid, Scopus and EMBASE via Elsevier were searched on 14th January 2022. An update was run on 16th June 2023. The search strategy focuses on concepts and keywords for disorders of consciousness and neurophysiological tools. The search strategy was developed with the support of a health sciences information specialist (MB) as recommended by the Cochrane Handbook for Systematic Reviews of Interventions[165]. The complete search strategy used for each database is listed in **Supplementary Tables 16-18**. The list of studies selected from the database search (see *Selection process*) was submitted to pDoC experts (OG, AT) to get recommendations of additional potentially eligible studies; the same list was also compared against the bibliographies of previously published literature reviews and meta-analyses on disorders of consciousness (by BK, SA, ZW, AS) to identify additional potentially eligible studies.

Selection process

The screening process was carried out using the platform Covidence[166]. Titles and abstracts of studies retrieved using the search strategy were reviewed manually (screening step #1). Studies passing the screening step #1 were reviewed manually based on full text and supplementary materials (screening step #2). Screening #1 and #2 was performed by at least two independent referees, among AS, MM, NA, SA, DS, BK, ZW and JA. Full-texts were automatically retrieved using Covidence and Zotero (https://www.zotero.org/); supplementary materials were automatically retrieved using the R package *suppdata* (https://github.com/ropensci/suppdata). Full-texts in non-English language (n=29) were translated using DeepL and a co-author fluent in Chinese (ZW, n=18), Russian (NB, n=6), German (AS, n=2) or Italian (AS, n=1); one Japanese (with tables and figures in English) and one Polish full-text were translated using DeepL only. Missing full-texts and/or information required for the screening process were requested from the study authors via email, phone and/or social media, in English or in the authors' mother tongue. If unrecoverable, information relative to inclusion criteria, and in particular to the proportion of adult (≥16 years old) or pDoC (≥28 days post-injury) patients in a given study, were estimated based on reported means and standard deviations, assuming a Gaussian distribution (n=3 with estimated proportion of pediatric DoC patients below 50% [range: 0-10%][53,63,106]; n=2 studies with estimated proportion of acute or subacute DoC patient below 50% [range: 3-6%][26,63]). Conflicts were resolved through discussion; a third referee (AS or JA) was brought into the discussion when necessary.

Data items extracted

The extraction process was carried out using the platform Covidence. A standardized form was used to extract data from the full text and supplementary materials passing screening step #2. Full-texts in non-English language (Chinese, n=4) were translated using DeepL and a co-author fluent in Chinese (ZW).

For EEG, MEG and fNIRS studies, we extracted the mean and standard deviations of any resting-state EEG, MEG or fNIRS global measure for pDoC, UWS/VS, MCS and healthy volunteers. If no data were available, they were requested from the study authors, as detailed above (n=67 studies, of which n=36 shared usable data). Whereby authors shared individual and/or electrode or source level data (n=14 studies), we computed the mean and standard deviation of the measures of interest across subjects, after averaging over channels/sources when necessary. All data received from the authors were inspected by MM and compared to the results reported in the original studies. Discrepancies were discussed with the authors, and if they could not be resolved, the data were excluded (n=3 studies). In case of no response, we pursued several strategies: (i) in case of data available in subgroups, we computed the combined mean and standard deviation of the pooled group of interest based on Cochrane's formulas[165] (n=30 studies); (ii) in case the median, interquartile range, minimum/maximum and/or standard error were available, we estimated the mean and standard deviation based on the formulas by Wan and colleagues[167] (n=0 studies); (iii) in case sufficient information was available in published plots, we used PlotDigitizer (https://plotdigitizer.com/) (n=13 studies) to extract the mean and standard deviation of groups (n=2 studies) and/or subgroups of interest (see strategy i, n=9 studies), or the individual values (n=2 studies), and/or the median, interquartile range, minimum/maximum and/or standard error (n=4 studies), from the high-resolution figures published in the full text or supplementary materials. The provenance of the statistics for each included study is detailed in **Supplementary Table 19**.

For PET, SPECT and MRI studies, we extracted the MNI or Talairach x, y and z peak coordinates of significant voxel-wise differences in resting-state PET, SPECT or MRI measures, between pDOC, UWS/VS or MCS against healthy volunteers and against each other. If no coordinates were reported, they were requested from the study authors (n=20 studies, of which n=13 shared usable data), as detailed above. If authors shared data in the form of thresholded statistical maps (n=4 studies), we used the SPM12 *spm_max* function to extract peak coordinates, with default settings, i.e., three coordinates at least 8 mm apart extracted from each significant cluster. Whereby authors shared unthresholded statistical maps (n=2 studies), an intensity-based and cluster-extent based threshold was applied, as per the original study. If no cluster-extent based threshold was explicitly reported, we applied a cluster-extent based threshold of 100 voxels to reduce risk of false positives and decrease the noise in the meta-analytical input. All data received from the authors were inspected by AS and compared to the results reported in the original studies. Discrepancies were discussed with the authors, and if they could not be solved, the data were excluded (n=0 studies). Tailarach coordinates were converted to MNI space (n=4 studies). The provenance of the statistics for each included study is detailed in **Supplementary Table 20 and 21**.

For all studies, we extracted information on overlap with previous studies and quality of evidence. We also extracted information relative to participants number, demographics (age, sex), clinics (diagnostic procedure and diagnosis, etiology and disease duration), data acquisition (time, center, neurophysiological tools and participants' set-up, including sedation), data processing and quantification, and statistical comparisons and thresholding. Summary descriptive statistics for demographic and clinical

information were computed as cumulative frequencies for qualitative variables, and mean and standard deviation of the cumulative Gaussian probability density function for quantitative variables (in-house code will be made available on GitHub, https://github.com/GIGA-Consciousness). The Gaussian probability density functions were estimated based on mean, standard deviation and minimum and maximum of each study; if minimum and maximum were not available, they were estimated based on the study mean ± 3*standard deviation (capped to the extreme minimum and maximum reported in the remaining studies). Statistical comparisons relative to qualitative variables were carried out based on Pearson's Chi-square test. Statistical comparisons relative to quantitative variables were carried out based on two-sample t-tests, after testing for equality of variances based on the F-test. Effect size was computed based on Hedges' g. All descriptive statistics and statistical tests were computed using the SciPy package in Python 3.12.

Quality of evidence, risk of bias and heterogeneity

Quality of evidence was evaluated based on a modified version of the NOS for case control studies, covering bias in selection, comparability and exposure (**Supplementary Table 1**).

For EEG, MEG and fNIRS studies, we evaluated heterogeneity based on the Cochran's Q test and the I^2 statistic. Publication bias due to missing results was evaluated whenever appropriate based on funnel plots and the Pustejovsky and Rodgers' modified version of the Egger's test[109] (for comparisons based on at least ten studies[165]), using the R package *meta*. We ran the modified version instead of the original as the latter has been shown to be more prone to Type I errors[168]. The Trim and Fill method was applied to assess the influence of publication bias on the pooled effect size.

For PET, SPECT and MRI studies, we evaluated heterogeneity in each meta-analytical cluster, based on an analysis of contributions, where the average non-linear contribution of each experiment is tested via a jack-knife approach. Risk of bias due to missing results was not evaluated, as the latter is designed for meta-analysis of effect sizes rather than of spatial consistency, where the research question is *whether* an effect is present, rather than *where* it is present.

Meta-analysis of global electrophysiological features

Meta-analysis of EEG, MEG and fNIRS findings was performed to evaluate the magnitude of the effect of neurophysiological findings in studies of pDOC, UWS/VS, MCS and/or healthy volunteers. Because heterogeneity was a priori expected, we used a random-effects meta-analysis via the R package *meta*. Classical inverse variance random-effects meta-analyses were applied with restricted maximum likelihood tau estimator, as per default settings. Effect sizes were computed using Hedges' g, corresponding to the mean difference divided by the pooled and weighted standard deviation. Results were deemed significant at $p<0.05$.

Mean and standard deviation of any EEG, MEG and fNIRS features were included in separate meta-analyses, provided the measure of interest was computed at global level (i.e., based on signal of usable electrodes placed across the entire scalp). Global features were grouped together into subfamilies of analogous EEG features, belonging to six families (power spectral density, connectivity, graph theory, microstates, entropy and complexity) and six bands (delta, theta, alpha, beta, gamma or broadband). The *power spectral density* family included features describing the distribution of the signal's frequency

contents; the *connectivity* family included features of phase and/or amplitude synchronization across brain locations; the *graph theory* family, split in different subfamilies, each including features reflecting a specific aspect of connectivity-derived brain network organization; the *microstate* family included features related to transient, quasi-stable topographical patterns of brain activity; the *entropy* family included features quantifying the unpredictability of the signal, and the *complexity* family included features relative to the degree of organization and amount of information necessary to describe the signal (**Supplementary Table 2**).

The primary comparisons of interest were pDoC patients against healthy controls, and UWS/VS patients against MCS patients. Secondary comparisons of interest were UWS patients against healthy controls, MCS patients against healthy controls and MCS subgroups (MCS-/MCS+) against any other group. We ran a meta-analysis for each individual subfamily of global features for which at least five different studies in independent clinical samples were available, according to best practices[108]. This resulted in meta-analysis of at least one subfamily of interest for each primary and secondary comparison of interest, with the exception of comparisons with MCS subgroups, for which not enough studies were available. Known overlaps in clinical samples within the same studies (i.e., in case of multi-measure studies) and across studies (i.e., in case of repeated inclusion of the same patients) were dealt with by excluding overlapping studies and testing robustness of the results by means of sensitivity analyses. Sensitivity analyses were run to evaluate the robustness of the meta-analysis results to inclusion/exclusion of (i) specific EEG sub-bands (when data on multiple sub-bands were reported in the same patients), (ii) specific EEG features (when data on multiple EEG, MEG and fNIRS features of the same family were reported in the same patients), (iii) markers obtained from imputation (e.g., mean obtained from the median; mean and standard deviation computed from extraction of data from published charts), (iv) clinical subpopulation with suspected covert consciousness and (v) presence of outliers (by leave-one-out sensitivity analysis), defined based on visual evaluation of the forest plots.

Coordinate-based meta-analysis of functional, structural and molecular neuroimaging findings

Coordinate-based meta-analysis of PET, SPECT and MRI findings was performed to evaluate the spatial consistency of neuroimaging findings in studies comparing pDOC, UWS/VS or MCS against healthy volunteers and against each other, using a random-effects analysis of convergence over experiments[16,169], i.e., comparisons of interest for which at least a coordinate is reported by a given study. Coordinate-based meta-analysis was performed via activation likelihood estimation, by means of in-house MATLAB code. In ALE, coordinates (also called foci) in 3-dimensional MNI or Talairach stereotactic space, obtained from different studies, are spatially normalized to a single template and smoothed with a Gaussian kernel to account for spatial uncertainty. The smoothing kernel dimensions are determined by the sample size of the experiment. The activation likelihood of each voxel is computed based on the union of the smoothed values, indicating the probability that at least one of 'true' peak activations lies within this voxel[16,169]. Results were deemed significant at a cluster-level $p<0.05$ FWE-corrected statistical threshold and a voxel-level uncorrected $p<0.001$ cluster-forming threshold.

Coordinates derived from comparison of any PET, SPECT and MRI measure were included in the meta-analysis, provided the comparisons were run at whole-brain level (i.e., including the telencephalon at the minimum, whereby brainstem and cerebellum might not have been included).

We considered both comparisons of decreased cerebral integrity (e.g., decreased gray matter density, metabolism, connectivity in patients compared to healthy volunteers) or relatively preserved cerebral

integrity. The primary comparisons of interest were decreases/relative preservation of cerebral integrity in pDoC patients against healthy controls, and UWS/VS patients against MCS patients. Secondary comparisons of interest were decreases/relative preservation of cerebral integrity in UWS/VS patients against healthy controls, MCS patients against healthy controls and in subgroups of MCS (MCS-/MCS+) against any other group. We ran coordinate-based meta-analysis for comparisons for which at least 20 experiments were available, according to best practices[111]. This resulted in a meta-analysis for the primary comparison of loss of cerebral integrity in pDoC patients against healthy controls. We further report exploratory results of coordinate-based meta-analysis for comparisons for which at least 10 experiments were available[170]. This resulted in exploratory meta-analyses of relative preservation of cerebral integrity in pDoC patients against healthy controls and decreased cerebral integrity in UWS/VS against MCS patients (primary comparisons), and in UWS/VS and MCS patients, respectively, against healthy controls (secondary comparisons). An insufficient number of studies was available for running meta-analyses of MCS- and MCS+ subgroups. Known overlaps in clinical samples within the same studies (i.e., in case of multimodal studies) and across studies (i.e., in case of repeated inclusion of the same patients) were treated by pooling the coordinates within the same experiment. Tags were included in the ALE input to evaluate the contribution of specific clinical sub-populations (UWS/VS, MCS) and imaging modalities (PET/SPECT, sMRI, fMRI) to the results. Sensitivity analyses were performed on unpooled coordinates to evaluate the impact of sample overlap on the main results via contribution analysis, for coordinates of any imaging modality and separately for coordinates of each imaging modality. We characterize the topography of meta-analytical findings using the REX toolbox (https://web.mit.edu/swg/software.htm), and (i) the Consensual Atlas of REsting-state Networks (CAREN)[171], (ii) the Human Connectome project multi-modal cortical parcellation 1.0 (HCP-MMPI) atlas[172], (iii) the Morel histological atlas of the human thalamus[173] and (iv) the 7-subdivision PET-MRI probabilistic atlas of the striatum[134].

Spatial correlation with an independent panel of multi-level neurobiological data

Following a similar rationale to the one recently proposed by[174], we relied on an unthresholded voxel-wise map of Z-statistics generated by ALE for the primary comparisons of interest and assessed their spatial correlation with an independent panel of multi-level neurobiological data, consisting of 65 different brain maps. Neurobiological brain maps were selected from the Neuromaps toolbox database (https://netneurolab.github.io/neuromaps). Only brain maps with data available for both hemispheres and generated based on data in at least n=10 observations were included; cortical surface maps were excluded when the same data were already available in the form of a whole-brain volume; whole-brain volumes were excluded when based on low-resolution imaging data (SPECT). This resulted in a final database of 28 cortical surfaces of microstructure, functional MRI connectivity, electrophysiology, developmental and evolutionary expansion and functional organization deriving from a total of 2,592 observations, and 37 whole-brain volumes of neural activity, neurotransmission, microglia and functional organization deriving from a total of 2,623 observations (not counting the functional organization derived from the Neurosynth meta-analytical database of 14,371 studies).

We performed spatial transformation, spatial correlation and significance testing based on comparison to a spatial null distribution using the Neuromaps toolbox (version 0.0.5) running on the GIGA high-performance computing (HPC) system (https://giga-bioinfo.gitlabpages.uliege.be/docs/mass-storage-

and-cluster/cluster/overview.html)[175]. Due to the extreme computational load of some of the algorithms used for computation of spatial nulls for brain volumes, we down-sampled the unthresholded ALE voxel-wise map of Z-statistics (source map) from a spatial resolution of 2 mm to 3 mm. The procedure ensures computational sustainability without affecting the results of the statistical comparisons neither for surface nor for volume target maps, as demonstrated by the almost perfect correlation (Pearson's R≈1) between p-values obtained from the source map of 2 mm vs. 3 mm (data available upon request). The source map was then transformed into the native space of each of the 65 multimodal brain maps (target maps), to which it was correlated. Significance of Pearson's correlations was (spin-)tested against two-sided spatial autocorrelation-preserving null models. Results were considered significant at $p<0.05$, Bonferroni-corrected for multiple comparisons within map-type. For surface target maps, we generated spatial nulls by means of the Alexander-Bloch method, that generates spatially-constrained null distributions by applying random rotations to spherical projects of the brain[176]. For volume target maps, we generated spatial nulls by means of the Burt method, that generates spatially-constrained null distributions by source-to-nulls variogram-matching, in order to retain the spatial autocorrelation of the original source map[177]. We used an optimized knn parameter (knn=800), determined via visual inspection of the fit between source and nulls variograms generated with knn parameters in the range of 500 to 16,000 using BrainSMASH 0.11.0[177]. Because of a possibly higher likelihood of false positives shown by the Burt method (demonstrated for parcellated surface data by Markello and colleagues[178]), we cross-validated our findings by generating spatial nulls by means of the Moran method[179], that generates spatially-constrained null distributions by using a spatial eigenvector as an estimate of spatial autocorrelation. For each map and method, we generated a minimum of 1,000 null maps, which were then correlated with the source maps to provide a null distribution of correlation coefficients, and estimated a two-tailed p-value for the original correlation. The exact number of null maps generated for each map and method was defined by first estimating the two-tailed p-value based on 1,000 null maps and its 95% Wilson confidence interval based on the binomial distributions[180]. If the target p-value fell within this 95% confidence interval, a more precise estimation was performed based on >1,000 maps. The number of null maps used finally varied from 1,000 to 50,000, depending on map and method. This procedure allows for a flexible, efficient use of computational resources, while ensuring a robust assessment of statistical significance in statistical frameworks where null distributions are randomly generated.

Data availability

Data generated during the study will be made available in the Zenodo repository (https://zenodo.org/). Code used in the study will be made available on GitHub (https://github.com/GIGA-Consciousness).

References

1. Di Perri, C. *et al.* Neural correlates of consciousness in patients who have emerged from a minimally conscious state: A cross-sectional multimodal imaging study. *Lancet Neurol.* **15**, 830–842 (2016).
2. Greene, D. J. *et al.* Integrative and Network-Specific Connectivity of the Basal Ganglia and Thalamus Defined in Individuals. *Neuron* **105**, 742-758.e6 (2020).
3. Tam, J. *et al.* Impact of coma duration on functional outcomes at discharge and long-term survival after cardiac arrest. *Resuscitation* **206**, 110444 (2025).
4. Rohaut, B. *et al.* Multimodal assessment improves neuroprognosis performance in clinically unresponsive critical-care patients with brain injury. *Nat. Med.* **30**, 2349–2355 (2024).
5. Seth, A. K. & Bayne, T. Theories of consciousness. *Nat. Rev. Neurosci.* **23**, 439–452 (2022).
6. Boly, M. *et al.* Are the neural correlates of consciousness in the front or in the back of the cerebral cortex? Clinical and neuroimaging evidence. *J. Neurosci.* **37**, 9603–9613 (2017).
7. Schiff, N. D. Mesocircuit mechanisms in the diagnosis and treatment of disorders of consciousness. *Press. Medicale* **52**, (2023).
8. Kondziella, D. *et al.* European Academy of Neurology guideline on the diagnosis of coma and other disorders of consciousness. *Eur. J. Neurol.* **27**, 741–756 (2020).
9. Nilsen, A. S., Juel, B., Thürer, B. & Storm, J. F. Proposed EEG measures of consciousness: a systematic, comparative review. (2020) doi:10.31234/osf.io/sjm4a.
10. Payen, J.-F., Schilte, C., Bertrand, B. & Behouche, A. Toward individualized sedation in patients with acute brain damage. *Anaesth. Crit. Care Pain Med.* **42**, 101219 (2023).
11. Kowalski, R. G. *et al.* Recovery of Consciousness and Functional Outcome in Moderate and Severe Traumatic Brain Injury. *JAMA Neurol.* **78**, 548–557 (2021).
12. Sala, A., Gosseries, O., Laureys, S. & Annen, J. Advances in neuroimaging in disorders of consciousness. *Handb. Clin. Neurol.* **207**, 97–127 (2025).
13. Hermann, B. *et al.* Combined behavioral and electrophysiological evidence for a direct cortical effect of prefrontal tDCS on disorders of consciousness. *Sci. Rep.* **10**, 4323 (2020).
14. Chennu, S. *et al.* Spectral Signatures of Reorganised Brain Networks in Disorders of Consciousness. *PLoS Comput. Biol.* **10**, (2014).
15. Gurevitch, J., Koricheva, J., Nakagawa, S. & Stewart, G. Meta-analysis and the science of research synthesis. *Nature* **555**, 175–182 (2018).
16. Eickhoff, S. B. *et al.* Coordinate-based activation likelihood estimation meta-analysis of neuroimaging data: A random-effects approach based on empirical estimates of spatial uncertainty. *Hum. Brain Mapp.* **30**, 2907–2926 (2009).
17. Kazazian, K., Monti, M. M. & Owen, A. M. Functional neuroimaging in disorders of consciousness: towards clinical implementation. *Brain* (2025) doi:10.1093/brain/awaf075.
18. Bareham, C. A. *et al.* Bedside EEG predicts longitudinal behavioural changes in disorders of consciousness. *NeuroImage Clin.* **28**, 102372 (2020).
19. Martens, G. *et al.* Behavioral and electrophysiological effects of network-based frontoparietal tDCS in patients with severe brain injury: A randomized controlled trial. *NeuroImage Clin.* **28**, (2020).
20. Bai, Y., Xia, X., Wang, Y., He, J. & Li, X. Assessment effects of repetitive transcranial magnetic stimulation in patients with disorders of consciousness by EEG. *Chinese J. Biomed. Eng.* **38**, 687–694 (2019).
21. Bai, Y., Xia, X., Wang, Y., He, J. & Li, X. Electroencephalography quadratic phase self-coupling correlates with consciousness states and restoration in patients with disorders of consciousness. *Clin. Neurophysiol.* **130**, 1235–1242 (2019).
22. Mortaheb, S. *et al.* A Graph Signal Processing Approach to Study High Density EEG Signals in

Patients with Disorders of Consciousness. *Annu. Int. Conf. IEEE Eng. Med. Biol. Soc. IEEE Eng. Med. Biol. Soc. Annu. Int. Conf.* **2019**, 4549–4553 (2019).
23. Lee, H. *et al.* Relationship of critical dynamics, functional connectivity, and states of consciousness in large-scale human brain networks. *Neuroimage* **188**, 228–238 (2019).
24. Cacciola, A. *et al.* Functional brain network topology discriminates between patients with minimally conscious state and unresponsivewakefulness syndrome. *J. Clin. Med.* **8**, (2019).
25. Rizkallah, J. *et al.* Decreased integration of EEG source-space networks in disorders of consciousness. *NeuroImage Clin.* **23**, 101841 (2019).
26. Engemann, D. A. *et al.* Robust EEG-based cross-site and cross-protocol classification of states of consciousness. *Brain* 1–14 (2018) doi:10.1093/brain/awy251.
27. Naro, A. *et al.* Bridging the Gap Towards Awareness Detection in Disorders of Consciousness: An Experimental Study on the Mirror Neuron System. *Brain Topogr.* **31**, 623–639 (2018).
28. Thibaut, A. *et al.* Preservation of brain activity in unresponsive patients identifies MCS star. *Ann. Neurol.* **90**, 89–100 (2021).
29. Naro, A. *et al.* Shedding new light on disorders of consciousness diagnosis: The dynamic functional connectivity. *Cortex* **103**, 316–328 (2018).
30. Wu, M. *et al.* Effect of acoustic stimuli in patients with disorders of consciousness: A quantitative electroencephalography study. *Neural Regen. Res.* **13**, 1900–1906 (2018).
31. Golkowski, D. *et al.* Simultaneous EEG–PET–fMRI measurements in disorders of consciousness: an exploratory study on diagnosis and prognosis. *J. Neurol.* **264**, 1986–1995 (2017).
32. Chennu, S. *et al.* Brain networks predict metabolism, diagnosis and prognosis at the bedside in disorders of consciousness. *Brain* **140**, 2120–2132 (2017).
33. Naro, A. *et al.* How far can we go in chronic disorders of consciousness differential diagnosis? The use of neuromodulation in detecting internal and external awareness. *Neuroscience* **349**, 165–173 (2017).
34. Xia, X. *et al.* Long-lasting repetitive transcranial magnetic stimulation modulates electroencephalography oscillation in patients with disorders of consciousness. *Neuroreport* **28**, 1022–1029 (2017).
35. Naro, A., Bramanti, P., Leo, A., Russo, M. & Calabrò, R. S. Transcranial Alternating Current Stimulation in Patients with Chronic Disorder of Consciousness: A Possible Way to Cut the Diagnostic Gordian Knot? *Brain Topogr.* **29**, 623–644 (2016).
36. Hao, X. *et al.* Correlation analysis of nonlinear characteristics in EEG with CRS-R score and visual characterization of rehabilitation process in DOC patients. *Chinese J. Biomed. Eng.* **34**, 153–159 (2015).
37. Marinazzo, D. *et al.* Directed information transfer in scalp electroencephalographic recordings: Insights on disorders of consciousness. *Clin. EEG Neurosci.* **45**, 33–39 (2014).
38. Lechinger, J. *et al.* CRS-R score in disorders of consciousness is strongly related to spectral EEG at rest. *J. Neurol.* **260**, 2348–2356 (2013).
39. Riganello, F. *et al.* The timecourse of electrophysiological brain–heart interaction in doc patients. *Brain Sci.* **11**, (2021).
40. Sarà, M. *et al.* Functional isolation within the cerebral cortex in the vegetative state: A nonlinear method to predict clinical outcomes. *Neurorehabil. Neural Repair* **25**, 35–42 (2011).
41. Sarà, M. & Pistoia, F. Complexity loss in physiological time series of patients in a vegetative state. *Nonlinear Dynamics. Psychol. Life Sci.* **14**, 1–13 (2010).
42. Yuan, Y., Liu, L., Qu, Y.-P., Wang, J. & Wu, D.-Y. Analysis and study of the effect of acupuncture on patients with different disturbance of consciousness using nonlinear dynamics of electroencephalography. *Chinese J. Cerebrovasc. Dis.* **6**, 461–465 (2009).
43. van den Brink, R. L. *et al.* Task-free spectral EEG dynamics track and predict patient recovery from

severe acquired brain injury. *NeuroImage. Clin.* **17**, 43–52 (2018).
44. Carriere, M. *et al.* Auditory localization should be considered as a sign of minimally conscious state based on multimodal findings. *Brain Commun.* **2**, fcaa195 (2020).
45. Wei, X. *et al.* Characterization of Spatial Temporal Dynamic of Brain Network in Disorder of Consciousness via Community Analysis. in *Chinese Control Conf., CCC* vols 2020-July 3168–3173 (IEEE Computer Society, 2020).
46. Liu, Y. *et al.* EEG complexity correlates with residual consciousness level of disorders of consciousness. *BMC Neurol.* **23**, (2023).
47. Maschke, C., Duclos, C., Owen, A. M., Jerbi, K. & Blain-Moraes, S. Aperiodic brain activity and response to anesthesia vary in disorders of consciousness. *Neuroimage* **275**, (2023).
48. Rosenfelder, M. J. *et al.* Effect of robotic tilt table verticalization on recovery in patients with disorders of consciousness: a randomized controlled trial. *J. Neurol.* **270**, 1721–1734 (2023).
49. Toplutaş, E., Aydın, F. & Hanoğlu, L. EEG Microstate Analysis in Patients with Disorders of Consciousness and Its Clinical Significance. *Brain Topogr.* (2023) doi:10.1007/s10548-023-00939-y.
50. Liu, B. *et al.* Outcome Prediction in Unresponsive Wakefulness Syndrome and Minimally Conscious State by Non-linear Dynamic Analysis of the EEG. *Front. Neurol.* **12**, (2021).
51. Chen, C. *et al.* Dynamic Changes of Brain Activity in Different Responsive Groups of Patients with Prolonged Disorders of Consciousness. *Brain Sci.* **13**, (2023).
52. Buccellato, A. *et al.* Disrupted relationship between intrinsic neural timescales and alpha peak frequency during unconscious states – A high-density EEG study. *Neuroimage* **265**, (2023).
53. Zhang, C. *et al.* The temporal dynamics of Large-Scale brain network changes in disorders of consciousness: A Microstate-Based study. *CNS Neurosci. Ther.* **29**, 296–305 (2023).
54. Helmstaedter, C. *et al.* Stimulation-related modifications of evolving functional brain networks in unresponsive wakefulness. *Sci. Rep.* **12**, (2022).
55. Han, J. *et al.* Functional Connectivity Increases in Response to High-Definition Transcranial Direct Current Stimulation in Patients with Chronic Disorder of Consciousness. *Brain Sci.* **12**, (2022).
56. Porcaro, C. *et al.* Fractal Dimension Feature as a Signature of Severity in Disorders of Consciousness: An EEG Study. *Int. J. Neural Syst.* **32**, (2022).
57. Guo, Y. *et al.* Dynamic Changes of Brain Activity in Patients With Disorders of Consciousness During Recovery of Consciousness. *Front. Neurosci.* **16**, (2022).
58. Han, J. *et al.* High-Definition Transcranial Direct Current Stimulation of the Dorsolateral Prefrontal Cortex Modulates the Electroencephalography Rhythmic Activity of Parietal Occipital Lobe in Patients With Chronic Disorders of Consciousness. *Front. Hum. Neurosci.* **16**, (2022).
59. Hao, Z., Xia, X., Bai, Y., Wang, Y. & Dou, W. EEG Evidence Reveals Zolpidem-Related Alterations and Prognostic Value in Disorders of Consciousness. *Front. Neurosci.* **16**, (2022).
60. Visani, E. *et al.* Entropy Metrics Correlating with Higher Residual Functioning in Patients with Chronic Disorders of Consciousness. *Brain Sci.* **12**, (2022).
61. Zilio, F. *et al.* Are intrinsic neural timescales related to sensory processing? Evidence from abnormal behavioral states. *Neuroimage* **226**, (2021).
62. Chen, L., Shang, L., Chunguang, C., Jiang, W. & Lihui, C. Spatiotemporal electroencephalography microstate analysis in disorders of consciousness. in *Chinese Control Conf., CCC* vols 2022-July 3008–3013 (IEEE Computer Society, 2022).
63. Zhuang, W. *et al.* Disrupted Control Architecture of Brain Network in Disorder of Consciousness. *IEEE Trans. Neural Syst. Rehabil. Eng.* **30**, 400–409 (2022).
64. Lee, M. *et al.* Quantifying arousal and awareness in altered states of consciousness using interpretable deep learning. *Nat. Commun.* **13**, 1–14 (2022).
65. Lutkenhoff, E. S. *et al.* EEG Power spectra and subcortical pathology in chronic disorders of

consciousness. *Psychol. Med.* 1–10 (2020) doi:10.1017/S003329172000330X.
66. Zhang, R. *et al.* Effects of High-Definition Transcranial Direct-Current Stimulation on Resting-State Functional Connectivity in Patients With Disorders of Consciousness. *Front. Hum. Neurosci.* **14**, (2020).
67. Wang, Y. *et al.* Spinal cord stimulation modulates complexity of neural activities in patients with disorders of consciousness. *Int. J. Neurosci.* **130**, 662–670 (2020).
68. Gui, P. *et al.* Assessing the depth of language processing in patients with disorders of consciousness. *Nat. Neurosci.* **23**, 761–770 (2020).
69. Kim, Y. W., Kim, H. S. & An, Y. S. Brain metabolism in patients with vegetative state after post-resuscitated hypoxic-ischemic brain injury: Statistical parametric mapping analysis of F-18 fluorodeoxyglucose positron emission tomography. *Chin. Med. J. (Engl).* **126**, 888–894 (2013).
70. Bruno, M. A. *et al.* Functional neuroanatomy underlying the clinical subcategorization of minimally conscious state patients. *J. Neurol.* **259**, 1087–1098 (2012).
71. Thibaut, A. *et al.* Metabolic activity in external and internal awareness networks in severely brain-damaged patients. *J. Rehabil. Med.* **44**, 487–494 (2012).
72. Kim, Y. W., Kim, H. S., An, Y.-S. & Im, S. H. Voxel-based statistical analysis of cerebral glucose metabolism in patients with permanent vegetative state after acquired brain injury. *Chin. Med. J. (Engl).* **123**, 2853–2857 (2010).
73. Juengling, F. D., Kassubek, J., Huppertz, H. J., Krause, T. & Els, T. Separating functional and structural damage in persistent vegetative state using combined voxel-based analysis of 3-D MRI and FDG-PET. *J. Neurol. Sci.* **228**, 179–184 (2005).
74. Kassubek, J. *et al.* Activation of a residual cortical network during painful stimulation in long-term postanoxic vegetative state: A 15O-H2O PET study. *J. Neurol. Sci.* **212**, 85–91 (2003).
75. Stender, J. *et al.* Quantitative rates of brain glucose metabolism distinguish minimally conscious from vegetative state patients. *J. Cereb. Blood Flow Metab.* **35**, 58–65 (2015).
76. Bruno, M.-A. *et al.* Visual fixation in the vegetative state: an observational case series PET study. *BMC Neurol.* **10**, 35 (2010).
77. He, Z. *et al.* Brain Metabolic Connectivity Patterns in Patients with Prolonged Disorder of Consciousness after Hypoxic-Ischemic Injury: A Preliminary Study. *Brain Sci.* **12**, (2022).
78. Sattin, D. *et al.* Visual behaviors in disorders of consciousness: Disentangling conscious visual processing by a multimodal approach. *Eur. J. Neurosci.* **52**, 4345–4355 (2020).
79. Aubinet, C. *et al.* Brain Metabolism but Not Gray Matter Volume Underlies the Presence of Language Function in the Minimally Conscious State (MCS): MCS+ Versus MCS− Neuroimaging Differences. *Neurorehabil. Neural Repair* **34**, 172–184 (2020).
80. Zhang, Y. *et al.* Neural correlates of different behavioral response to transcranial direct current stimulation between patients in the unresponsive wakefulness syndrome and minimally conscious state. *Neurol. Sci.* **41**, 75–82 (2020).
81. Mortensen, K. N. *et al.* Impact of global mean normalization on regional glucose metabolism in the human brain. *Neural Plast.* **2018**, (2018).
82. Rosazza, C. *et al.* Multimodal study of default-mode network integrity in disorders of consciousness. *Ann. Neurol.* **79**, 841–853 (2016).
83. Chatelle, C. *et al.* Changes in cerebral metabolism in patients with a minimally conscious state responding to zolpidem. *Front. Hum. Neurosci.* (2014) doi:10.3389/fnhum.2014.00917.
84. Stender, J. *et al.* Diagnostic precision of PET imaging and functional MRI in disorders of consciousness: A clinical validation study. *Lancet* **384**, 514–22 (2014).
85. Juengling, F. D., Kassubek, J., Huppertz, H.-J., Krause, T. & Els, T. Separating functional and structural damage in persistent vegetative state using combined voxel-based analysis of 3-D MRI and FDG-PET. *J. Neurol. Sci.* **228**, 179–184 (2005).

86. Zhou, J. *et al.* Specific and nonspecific thalamocortical functional connectivity in normal and vegetative states. *Conscious. Cogn.* **20**, 257–268 (2011).
87. He, J.-H. *et al.* Hyperactive external awareness against hypoactive internal awareness in disorders of consciousness using resting-state functional MRI: Highlighting the involvement of visuo-motor modulation. *NMR Biomed.* **27**, 880–886 (2014).
88. Huang, Z. *et al.* The self and its resting state in consciousness: An investigation of the vegetative state. *Hum. Brain Mapp.* **35**, 1997–2008 (2014).
89. Demertzi, A. *et al.* Multiple fMRI system-level baseline connectivity is disrupted in patients with consciousness alterations. *Cortex* **52**, 35–46 (2014).
90. He, J. H. *et al.* Decreased functional connectivity between the mediodorsal thalamus and default mode network in patients with disorders of consciousness. *Acta Neurol. Scand.* **131**, 145–151 (2015).
91. Demertzi, A. *et al.* Intrinsic functional connectivity differentiates minimally conscious from unresponsive patients. *Brain* **138**, 2619–2631 (2015).
92. Wu, X. *et al.* Intrinsic functional connectivity patterns predict consciousness level and recovery outcome in acquired brain injury. *J. Neurosci.* **35**, 12932–12946 (2015).
93. Soddu, A. *et al.* Correlation between resting state fMRI total neuronal activity and PET metabolism in healthy controls and patients with disorders of consciousness. *Brain Behav.* **6**, 1–15 (2016).
94. Rosazza, C. *et al.* Multimodal study of default-mode network integrity in disorders of consciousness. *Ann. Neurol.* **79**, 841–853 (2016).
95. Kirsch, M. *et al.* Sedation of patients with disorders of consciousness during neuroimaging: Effects on resting state functional brain connectivity. *Anesth. Analg.* **124**, 588–598 (2017).
96. Aubinet, C. *et al.* Clinical subcategorization of minimally conscious state according to resting functional connectivity. *Hum. Brain Mapp.* **39**, 4519–4532 (2018).
97. Zhang, L. *et al.* Functional connectivity of anterior insula predicts recovery of patients with disorders of consciousness. *Front. Neurol.* **9**, (2018).
98. Kremneva, E. I. *et al.* Feasibility of non-gaussian diffusion metrics in chronic disorders of consciousness. *Brain Sci.* **9**, (2019).
99. Wu, X. *et al.* Spatially Overlapping Regions Show Abnormal Thalamo-frontal Circuit and Abnormal Precuneus in Disorders of Consciousness. *Brain Topogr.* **32**, 445–460 (2019).
100. Wu, G.-R. *et al.* Modulation of the spontaneous hemodynamic response function across levels of consciousness. *Neuroimage* **200**, 450–459 (2019).
101. Luppi, A. I. *et al.* Consciousness-specific dynamic interactions of brain integration and functional diversity. *Nat. Commun.* **10**, (2019).
102. Cao, B. *et al.* Time-delay structure predicts clinical scores for patients with disorders of consciousness using resting-state fMRI. *NeuroImage Clin.* **32**, (2021).
103. Boltzmann, M. *et al.* Auditory Stimulation Modulates Resting-State Functional Connectivity in Unresponsive Wakefulness Syndrome Patients. *Front. Neurosci.* **15**, (2021).
104. Yu, Y. *et al.* Disrupted Strength and Stability of Regional Brain Activity in Disorder of Consciousness Patients: A Resting-State Functional Magnetic Resonance Imaging Study. *Neuroscience* **469**, 59–67 (2021).
105. Wang, Y. *et al.* Regional Homogeneity Alterations in Patients with Impaired Consciousness. An Observational Resting-State fMRI Study. *Neuroradiology* **64**, 1391–1399 (2022).
106. Chen, W. *et al.* Functional differences in key brain regions in patients with different levels of consciousness after severe brain injury. *Chinese J. Neuromedicine* **21**, 593–599 (2022).
107. Di Perri, C. *et al.* Limbic hyperconnectivity in the vegetative state. *Neurology* **81**, 1417–1424 (2013).

108. Myung, S.-K. How to review and assess a systematic review and meta-analysis article. *Sci. Ed.* **10**, 119–126 (2023).
109. Pustejovsky, J. E. & Rodgers, M. A. Testing for funnel plot asymmetry of standardized mean differences. *Res. Synth. Methods* **10**, 57–71 (2019).
110. Kremneva, E. I. *et al.* Feasibility of non-gaussian diffusion metrics in chronic disorders of consciousness. *Brain Sci.* **9**, (2019).
111. Müller, V. I. *et al.* Ten simple rules for neuroimaging meta-analysis. *Neurosci. Biobehav. Rev.* **84**, 151–161 (2018).
112. Lopes Da Silva, F. H. & Storm Van Leeuwen, W. The cortical source of the alpha rhythm. *Neuroscience letters* vol. 6 237–241 (1977).
113. Burns, B. Y. B. D. Some properties of the cat's isolated cerebral cortex. *J. Physiol.* **3**, 50–68 (1950).
114. Amzica, F. & Steriade, M. Electrophysiological correlates of sleep delta waves. *Electroencephalogr. Clin. Neurophysiol.* **107**, 69–83 (1998).
115. Flint, A. C. & Connors, B. W. Two types of network oscillations in neocortex mediated by distinct glutamate receptor subtypes and neuronal populations. *J. Neurophysiol.* **75**, 951–957 (1996).
116. Hughes, S. W. *et al.* Synchronized oscillations at α and θ frequencies in the lateral geniculate nucleus. *Neuron* **42**, 253–268 (2004).
117. Silva, L. R., Amitai, Y. & Connors, B. W. Intrinsic oscillations of neocortex generated by layer 5 pyramidal neurons. *Science (80-.).* **251**, 432–435 (1991).
118. Florin, E. & Baillet, S. The brain's resting-state activity is shaped by synchronized cross-frequency coupling of neural oscillations. *Neuroimage* **111**, 26–35 (2015).
119. Jensen, O. *et al.* On the human sensorimotor-cortex beta rhythm: Sources and modeling. *Neuroimage* **26**, 347–355 (2005).
120. McCarthy, M. M. *et al.* Striatal origin of the pathologic beta oscillations in Parkinson's disease. *Proc. Natl. Acad. Sci. U. S. A.* **108**, 11620–11625 (2011).
121. Sherman, M. A. *et al.* Neural mechanisms of transient neocortical beta rhythms: Converging evidence from humans, computational modeling, monkeys, and mice. *Proc. Natl. Acad. Sci. U. S. A.* **113**, E4885–E4894 (2016).
122. Vanhaudenhuyse, A. *et al.* Two distinct neuronal networks mediate the awareness of environment and of self. *J. Cogn. Neurosci.* **23**, 570–578 (2011).
123. Mancuso, L. *et al.* Tasks activating the default mode network map multiple functional systems. *Brain Struct. Funct.* **227**, 1711–1734 (2022).
124. Wang, S., Tepfer, L. J., Taren, A. A. & Smith, D. V. Functional parcellation of the default mode network: a large-scale meta-analysis. *Sci. Rep.* **10**, (2020).
125. Aubinet, C., Vanhaudenhuyse, A., Laureys, S. & Demertzi, A. The self in disorders of consciousness. *Phenomenological neuropsychiatry: How patient experience bridges the clinic with clinical neuroscience.* 209–229 (2024) doi:10.1007/978-3-031-38391-5_16.
126. Menon, V. 20 years of the default mode network: A review and synthesis. *Neuron* **111**, 2469–2487 (2023).
127. Araujo, H. F., Kaplan, J., Damasio, H. & Damasio, A. Neural correlates of different self domains. *Brain Behav.* **5**, 1–5 (2015).
128. Luppi, A. I., Lyu, D. & Stamatakis, E. A. Core of consciousness: the default mode network as nexus of convergence and divergence in the human brain. *Curr. Opin. Behav. Sci.* **65**, 101545 (2025).
129. Herbet, G., Lemaitre, A. L., Moritz-Gasser, S., Cochereau, J. & Duffau, H. The antero-dorsal precuneal cortex supports specific aspects of bodily awareness. *Brain* **142**, 2207–2214 (2019).
130. Schiff, N. D. Central thalamic contributions to arousal regulation and neurological disorders of consciousness. *Ann. N. Y. Acad. Sci.* **1129**, 105–118 (2008).
131. Liu, M., Lerma-Usabiaga, G., Clascá, F. & Paz-Alonso, P. M. High-Resolution Tractography Protocol

to Investigate the Pathways between Human Mediodorsal Thalamic Nucleus and Prefrontal Cortex. *J. Neurosci.* **43**, 7780–7798 (2023).
132. Aggleton, J. P., Saunders, R. C., Wright, N. F. & Vann, S. D. The origin of projections from the posterior cingulate and retrosplenial cortices to the anterior, medial dorsal and laterodorsal thalamic nuclei of macaque monkeys. *Eur. J. Neurosci.* **39**, 107–123 (2014).
133. Harrison, B. J. *et al.* Dynamic subcortical modulators of human default mode network function. *Cereb. Cortex* **32**, 4345–4355 (2022).
134. Tziortzi, A. C. *et al.* Connectivity-Based Functional Analysis of Dopamine Release in the Striatum Using Diffusion-Weighted MRI and Positron Emission Tomography. *Cereb. Cortex* **24**, 1165–1177 (2013).
135. Johnson, T. N. Fiber connections between the dorsal thalamus and corpus striatum in the cat. *Exp. Neurol.* **3**, 556–569 (1961).
136. Tobias, T. J. Afferents to prefrontal cortex from the thalamic mediodorsal nucleus in the rhesus monkey. *Brain Res.* **83**, 191–212 (1975).
137. Parent, A., Mackey, A. & De Bellefeuille, L. The subcortical afferents to caudate nucleus and putamen in primate: A fluorescence retrograde double labeling study. *Neuroscience* **10**, 1137–1150 (1983).
138. Buckner, R. L. & Krienen, F. M. The evolution of distributed association networks in the human brain. *Trends Cogn. Sci.* **17**, 648–665 (2013).
139. Xu, T. *et al.* Cross-species functional alignment reveals evolutionary hierarchy within the connectome. *Neuroimage* **223**, 117346 (2020).
140. Grimm, C. *et al.* Tonic and burst-like locus coeruleus stimulation distinctly shift network activity across the cortical hierarchy. *Nat. Neurosci.* **27**, 2167–2177 (2024).
141. Ferguson, K. A. & Cardin, J. A. Mechanisms underlying gain modulation in the cortex. *Nat. Rev. Neurosci.* **21**, 80–92 (2020).
142. Dahl, M. J., Mather, M. & Werkle-Bergner, M. Noradrenergic modulation of rhythmic neural activity shapes selective attention. *Trends Cogn. Sci.* **26**, 38–52 (2022).
143. Vazey, E. M., Moorman, D. E. & Aston-Jones, G. Phasic locus coeruleus activity regulates cortical encoding of salience information. *Proc. Natl. Acad. Sci. U. S. A.* **115**, E9439–E9448 (2018).
144. Oyarzabal, E. A. *et al.* Chemogenetic stimulation of tonic locus coeruleus activity strengthens the default mode network. *Sci. Adv.* **8**, 1–12 (2022).
145. Steel, A., Mikkelsen, M., Edden, R. A. E. & Robertson, C. E. Regional balance between glutamate+glutamine and GABA+ in the resting human brain. *Neuroimage* **220**, (2020).
146. Gao, R., Peterson, E. J. & Voytek, B. Inferring synaptic excitation/inhibition balance from field potentials. *Neuroimage* **158**, 70–78 (2017).
147. Luppi, A. I. *et al.* In vivo mapping of pharmacologically induced functional reorganization onto the human brain's neurotransmitter landscape. *Sci. Adv.* **9**, (2023).
148. Liao, D., Lin, H., Ping, Y. L. & Loh, H. H. Mu-opioid receptors modulate the stability of dendritic spines. *Proc. Natl. Acad. Sci. U. S. A.* **102**, 1725–1730 (2005).
149. Jiang, Z. G. & North, R. A. Pre- and postsynaptic inhibition by opioids in rat striatum. *J. Neurosci.* **12**, 356–361 (1992).
150. Gomez-Mancilla, B. *et al.* Mavoglurant reduces cocaine use in patients with cocaine use disorder in a phase 2 clinical trial. *Sci. Transl. Med.* **17**, eadi4505 (2025).
151. Simpson, D. & Perry, C. M. Atomoxetine. *Pediatr. Drugs* **5**, 407–415 (2003).
152. Edlow, B. L. *et al.* Common Data Elements for Disorders of Consciousness: Recommendations from the Working Group on Neuroimaging. *Neurocrit. Care* **39**, 611–617 (2023).
153. Drohan, C. M. *et al.* Effect of sedation on quantitative electroencephalography after cardiac arrest. *Resuscitation* **124**, 132–137 (2018).

154. Barry, R. J. & De Blasio, F. M. EEG differences between eyes-closed and eyes-open resting remain in healthy ageing. *Biol. Psychol.* **129**, 293–304 (2017).
155. Riedl, V. *et al.* Local activity determines functional connectivity in the resting human brain: a simultaneous FDG-PET/fMRI study. *J. Neurosci.* **34**, 6260–6266 (2014).
156. Hannawi, Y., Lindquist, M., Caffo, B., Sair, H. & Stevens, R. Resting brain activity in disorders of consciousness. *Neurology* **84**, 1272–1280 (2015).
157. Kotchoubey, B. & Pavlov, Y. G. A systematic review and meta-analysis of the relationship between brain data and the outcome in disorders of consciousness. *Front. Neurol.* **9**, 1–15 (2018).
158. Giacino, J. T. *et al.* Practice guideline update recommendations summary: Disorders of consciousness. *Neurology* **91**, 450–460 (2018).
159. Song, M. *et al.* Prognostic models for prolonged disorders of consciousness: an integrative review. *Cell. Mol. Life Sci.* **77**, 3945–3961 (2020).
160. Mencarelli, L. *et al.* Network Mapping of Connectivity Alterations in Disorder of Consciousness: Towards Targeted Neuromodulation. *J. Clin. Med.* **9**, 828 (2020).
161. Page, M. J. *et al.* The PRISMA 2020 statement: An updated guideline for reporting systematic reviews. *BMJ* **372**, (2021).
162. The Multi-Scoeity Task Force on PVS. Medical aspects of the persistent vegetative state. *N. Engl. J. Med.* **330**, 1499–508 (1994).
163. Giacino, J. T. *et al.* Development of practice guidelines for assessment and management of the vegetative and minimally conscious states. *Journal of Head Trauma Rehabilitation* vol. 12 79–89 (1997).
164. Seel, R. T. *et al.* Assessment scales for disorders of consciousness: Evidence-based recommendations for clinical practice and research. *Arch. Phys. Med. Rehabil.* **91**, 1795–1813 (2010).
165. Higgins, J. *et al. Cochrane Handbook for Systematic Reviews of Interventions*. (Cochrane, 2024).
166. Covidence. Covidence systematic review software. *Covidence systematic review software, Veritas Health Innovation, Melbourne, Australia* (2023).
167. Wan, X., Wang, W., Liu, J. & Tong, T. Estimating the sample mean and standard deviation from the sample size, median, range and/or interquartile range. *BMC Med. Res. Methodol.* **14**, 1–13 (2014).
168. Zwetsloot, P. P. *et al.* Standardized mean differences cause funnel plot distortion in publication bias assessments. *Elife* **6**, 1–20 (2017).
169. Turkeltaub, P. E. *et al.* Minimizing within-experiment and within-group effects in activation likelihood estimation meta-analyses. *Hum. Brain Mapp.* **33**, 1–13 (2012).
170. Eickhoff, S. B. *et al.* Behavior, sensitivity, and power of activation likelihood estimation characterized by massive empirical simulation. *Neuroimage* **137**, 70–85 (2016).
171. Doucet, G. E., Lee, W. H. & Frangou, S. Evaluation of the spatial variability in the major resting-state networks across human brain functional atlases. *Hum. Brain Mapp.* **40**, 4577–4587 (2019).
172. Glasser, M. F. *et al.* A multi-modal parcellation of human cerebral cortex. *Nature* **536**, 171–178 (2016).
173. Krauth, A. *et al. A mean three-dimensional atlas of the human thalamus: Generation from multiple histological data*. *NeuroImage* vol. 49 (2010).
174. Larivière, S. *et al.* BrainStat: A toolbox for brain-wide statistics and multimodal feature associations. *Neuroimage* **266**, (2023).
175. Markello, R. D. *et al.* Neuromaps: Structural and Functional Interpretation of Brain Maps. *Nat. Methods* **19**, 1472–1479 (2022).
176. Alexander-Bloch, A. F. *et al.* On testing for spatial correspondence between maps of human brain

structure and function. *Neuroimage* **178**, 540–551 (2018).
177. Burt, J. B., Helmer, M., Shinn, M., Anticevic, A. & Murray, J. D. Generative modeling of brain maps with spatial autocorrelation. *Neuroimage* **220**, 117038 (2020).
178. Markello, R. D. & Misic, B. Comparing spatial null models for brain maps. *Neuroimage* **236**, 118052 (2021).
179. Wagner, H. H. & Dray, S. Generating spatially constrained null models for irregularly spaced data using Moran spectral randomization methods. Methods Ecol Evol 6: 1169–1178. *Methods Ecol. Evol.* **6**, 1169–1178 (2015).
180. Wilson, E. B. Probable inference, the law of succession, and statistical inference. *J. Am. Stat. Assoc.* **22**, 209–212 (1927).

Acknowledgements

We thank Dr. Tamás Koi and Ms. Lucija Anušić for their support. We thank all authors of studies screened and/or included in this meta-analysis for sharing essential information, namely E. Kondratyeva of A.L. Polenov Russian Scientific Research Institute; A. Fingerlkurts of BM Science; J. Hou and Y. Li of the China Academy of Chinese Medical Sciences; L. Wang and P. Gui of the Chinese Academy of Sciences; S. Stefan of the Dana-Farber Cancer Institute; D. Zang, Q. Zou, X. Wu, and Y. Mao of Fudan University; G. Marotta of IRCCS Ca' Granda Ospedale Maggiore Policlinico Milano; A. Cacciola, A. Naro, and R.S. Calabrò of IRCCS Centro Neurolesi "Bonino-Pulejo"; A. Nigri, A. Bersano, C. Rosazza, D. Sattin, F. Panzica, G. Varotto, G. Bedini, S.D. Rossi, S. Ferraro, and S. Franceschetti of IRCCS Istituto Neurologico Carlo Besta; E.A. Parati of IRCCS Maugeri Milano; M. Cavinato of IRCCS Ospedale San Camillo; E. Toplutas of Istanbul Medipol University; J. Long of Jinan University; C. Bareham of Massey University; C. Maschke and S. Blain-Moraes of McGill University; Z. Huang of the Michigan Neuroscience Institute; M. Hassan of MINDig; Y. Yang of the National Institutes of Health; Y. Wang and X. Li of Normal University of Beijing; B. Hermann, D.-A. Engemann, J. Sitt, and L. Naccache of the Paris Brain Institute; P.M. Rossini of Policlinico Gemelli; E.I. Kremneva of the Research Center of Neurology; F. Riganello of S. Anna Institute; B. Cao and R. Huang of South China Normal University; C. Cavaliere of Synlab; W.L. Magee of Temple University; M. Lee of The Catholic University of Korea; J. Han, K. Wang, and Y. Hu of The First Affiliated Hospital of Anhui Medical University; X. Xia and J. He of The Seventh Medical Center of the Chinese PLA General Hospital; A. Bender and M. Rosenfelder of Therapiezentrum Burgau; C. Chu of Tianjin University; W. Dou and Z. Hao of Tsinghua University; F. Gomez of Universidad Nacional de Colombia; F. Pistoia of Università degli Studi dell'Aquila; B. Hakiki of Università di Firenze; D. Golkowski of Universitätsklinikum Heidelberg; C. Di Perri of University Hospital Coventry and Warwickshire; R. Van den Brink of University Medical Center Hamburg-Eppendorf; F. Juengling of University of Alberta; S. Mortaheb of University of Antwerp; C. Helmstaedter, K. Lehnertz, T. Rings, and T. Bröhl of University of Bonn; E. Lutkenhoff of University of California, Los Angeles; R. Panda of University of California, San Francisco; A. Luppi, E.A. Stamatakis, T. Fryer, and V. Newcombe of University of Cambridge; J. Shock of University of Cape Town; J. Stender of University of Copenhagen; A. Grippo of University of Firenze; D. Marinazzo of University of Gent; S. Chennu and P. Ramaswamy of University of Kent; A. Demertzi, C. Aubinet, and G. Martens of University of Liège; U. Lee of University of Michigan Medical School; G. Northoff of University of Ottawa; A. Buccellato, C. Porcaro, E. Formaggio, F. Zilio, and F. Piccione of University of Padua; J. Rizkallah, J. Modolo, and P. Benquet of University of Rennes; J. Toppi and L. Astolfi of University of Rome "Sapienza"; T. Varley of the Vermont Complex Systems Institute; P. Guldenmund of Vrije Universiteit Amsterdam; I. Maximov of Western Norway University of Applied Sciences; D.-Y. Wu of Xuanwu Hospital of Capital Medical University; F. Hyder of Yale University; B. Luo, G. Pan, and X. Sun of Zhejiang University; Y. Hu of Zhengzhou University; and Q. Xie of Zhujiang Hospital. We also thank the patients and their families, and the control participants for taking part in all studies. The authors also acknowledge use of the GIGA high performance computing cluster for conducting the analysis reported in this paper.

The study was supported by the University and University Hospital of Liège, the Belgian National Funds for Scientific Research (FRS-FNRS), the FNRS PDR project (T.0134.21), the FNRS MIS project (F.4521.23), the FLAG-ERA JTC2021 project ModelDXConsciousness (Human Brain Project Partnering Project) and FLAG-ERA JTC 2023 - HBP - Basic and Applied Research, project BrainAct, JTC the fund Generet, the King Baudouin Foundation, the BIAL Foundation, the Mind Science Foundation, the Fondation Leon Fredericq, and the Horizon 2020 MSCA – Research and Innovation Staff Exchange DoC-Box project (HORIZON-MSCA-2022-SE-01-01; 101131344). SL is supported by the Canada Excellence Research Chair in Neuroplasticity, the Belgian National Fund for Scientific Research, the fund Generet of King Baudouin Foundation, the European Foundation for Biomedical Research and the National Natural Science Foundation of China.

OG and AT are research associates and SL research director at FRS-FNRS. JA is postdoctoral fellow at the FWO (1265522N).

Author contributions

A.S. contributed to conception, study design, data collection, extraction and analysis, interpretation and drafting the work; M.M. to data collection, extraction and analysis and revision; N.A. to data collection and extraction and revision; N.B. to study design, analysis and revision; S.A., D.S., B.K, Z.W. to data collection and extraction and revision; M.B. to search strategy and revision; C.B.; S.B.E. to study design and revision; D.M. to interpretation and revision; M.T. to study design and revision; S.L. to interpretation and revision; O.G. to study design and revision; A.T. to study design, interpretation and revision; J.A. to conception, study design, data collection, extraction and analysis, interpretation and revision.

Competing interest

The authors declare no competing interests.

Materials & Correspondence

Materials and correspondence should be addressed to Jitka Annen, Jitka.Annen@uliege.be, coma@uliege.be.

Table 1. Quality appraisal of included studies based on an adapted version of the NOS.

		Case definition	Case representativeness	Control selection	Control definition	Age	Sex	Ascertainment of exposure	
Tool	**Study**	**Selection**				**Comparability**		**Exposure**	**Total**
PET	Kassubek 2003	★	☆	☆	☆	☆	☆	★	★★
PET	Juengling 2005	★	☆	☆	☆	☆	☆	★	★★
PET	Bruno 2010	★	★	☆	☆	☆	☆	★	★★★☆☆
PET	Kim 2010	★	★	☆	☆	☆	☆	★	★★★☆☆
PET	Bruno 2012	★	☆	☆	☆	★	☆	★	★★★☆
PET	Thibaut 2012	★	★	☆	☆	☆	☆	★	★★★☆☆
PET	Kim 2013	★	★	☆	☆	☆	☆	★	★★★☆☆
PET	Chatelle 2014	★	☆	☆	☆	★	☆	★	★★★
PET	Stender 2014	★	★	☆	★	☆	☆	★	★★★★☆
PET	Mortensen 2018	★	☆	☆	☆	☆	☆	★	★★☆
PET	Aubinet 2020	★	★	☆	★	☆	☆	★	★★★★☆☆
PET	Carriere 2020	★	★	☆	☆	★	☆	★	★★★★☆
PET	Zhang 2020	★	★	☆	★	☆	☆	★	★★★★
PET	He 2022	★	☆	☆	☆	☆	☆	★	★★
MRI	Juengling 2005	★	☆	☆	★	☆	☆	★	★★★☆☆
MRI	Zhou 2011	★	☆	☆	★	☆	☆	★	★★★
MRI	DiPerri 2013	★	☆	☆	☆	★	★	★	★★★★
MRI	Demertzi 2014	★	★	☆	★	☆	☆	★	★★★★☆☆
MRI	He 2014	★	☆	☆	☆	☆	☆	★	★★☆☆
MRI	Huang 2014	★	☆	☆	☆	☆	☆	★	★★☆
MRI	He 2015	★	☆	☆	★	☆	☆	★	★★★☆☆
MRI	Wu 2015	★	★	☆	★	★	★	★	★★★★★★
MRI	Soddu 2016	★	☆	☆	☆	☆	☆	★	★★☆☆
MRI	Kirsch 2017	★	☆	☆	☆	☆	☆	★	★★☆
MRI	Aubinet 2018	★	★	☆	★	☆	☆	★	★★★★☆
MRI	Zhang 2018	★	☆	☆	☆	☆	☆	★	★★☆
MRI	Kremneva 2019	★	☆	☆	☆	☆	☆	★	★★☆☆
MRI	Luppi 2019	★	★	☆	★	☆	☆	★	★★★★☆
MRI	Wu 2019a	★	★	☆	★	☆	☆	★	★★★★☆
MRI	Wu 2019b	★	☆	☆	★	☆	☆	★	★★★☆☆
MRI	Aubinet 2020	★	☆	★	★	☆	☆	★	★★★★☆
MRI	Carriere 2020	★	★	☆	★	☆	☆	★	★★★★☆☆

MRI	Boltzmann 2021	★	☆	☆	☆	✯	☆	★	★★✯
MRI	Cao 2021	★	☆	☆	★	☆	✯	★	★★★✯
MRI	Yu 2021	★	★	☆	☆	✯	✯	★	★★★✯✯
EEG	Sarà 2010	★	☆	☆	☆	★	★	★	★★★★
EEG	Sarà 2011	★	★	★	★	★	★	★	★★★★★★★
EEG	Lechinger 2013	★	☆	☆	☆	✯	☆	★	★★✯
EEG	Chennu 2014	★	☆	☆	☆	☆	✯	★	★★✯
EEG	Marinazzo 2014	★	☆	☆	☆	★	✯	★	★★★✯
EEG	Naro 2016	★	★	☆	★	✯	✯	★	★★★★✯✯
EEG	Chennu 2017	★	★	☆	☆	☆	☆	★	★★★
EEG	Naro 2017	★	☆	☆	☆	★	✯	★	★★★✯
EEG	Naro 2018a	★	☆	☆	★	★	★	★	★★★★★
EEG	van den Brink 2018	★	☆	☆	☆	✯	✯	★	★★✯✯
EEG	Wu 2018	★	☆	☆	★	☆	✯	★	★★★✯
EEG	Bai 2019	★	☆	☆	☆	★	✯	★	★★★✯
EEG	Mortaheb 2019	★	☆	☆	★	✯	✯	★	★★★✯✯
EEG	Rizkallah 2019	★	☆	☆	☆	☆	☆	★	★★
EEG	Carriere 2020	★	★	☆	☆	✯	✯	★	★★★✯✯
EEG	Gui 2020	★	★	☆	☆	☆	☆	★	★★★
EEG	Wei 2020	★	☆	☆	☆	☆	☆	★	★★
EEG	Riganello 2021	★	☆	☆	☆	☆	✯	★	★★✯
EEG	Thibaut 2021	★	☆	☆	☆	★	☆	★	★★★
EEG	Zilio 2021	★	☆	☆	☆	✯	✯	★	★★✯✯
EEG	Chen 2022	★	☆	☆	☆	☆	☆	★	★★
EEG	Hao 2022	★	☆	☆	☆	★	★	★	★★★★
EEG	Helmstaedter 2022	★	★	☆	☆	☆	✯	★	★★★✯
EEG	Lee 2022	★	☆	☆	☆	☆	☆	★	★★
EEG	Porcaro 2022	★	☆	☆	☆	☆	✯	★	★★✯
EEG	Zhuang 2022	★	☆	☆	★	☆	✯	★	★★★✯
EEG	Buccellato 2023	★	☆	☆	☆	☆	☆	★	★★
EEG	Liu 2023	★	☆	☆	☆	☆	☆	★	★★
EEG	Toplutas 2023	★	☆	☆	☆	✯	✯	★	★★✯✯
Studies not including healthy controls for meta-analysis									
PET	Stender 2015	★	☆					★	★★
PET	Rosazza 2016	★	★					★	★★★
PET	Golkowski 2017	★	★					★	★★★
PET	Sattin 2020	★	★					★	★★★
PET	Thibaut 2021	★	★					★	★★★
MRI	Demertzi 2015	★	☆					★	★★
MRI	Rosazza 2016	★	★					★	★★★
MRI	Thibaut 2021	★	☆					★	★★

MRI	Chen 2022	★	★		★	★★★
MRI	Wang 2022	★	★		★	★★★
EEG	Yuan 2009	★	★		★	★★★
EEG	Hao 2015	★	★		★	★★★
EEG	Golkowski 2017	★	★		★	★★★
EEG	Xia 2017	★	★		★	★★★
EEG	Engemann 2018	★	☆		★	★★
EEG	Naro 2018a	★	★		★	★★★
EEG	Bai 2019	★	☆		★	★★
EEG	Cacciola 2019	★	★		★	★★★
EEG	Lee 2019	★	☆		★	★★
EEG	Bareham 2020	★	★		★	★★★
EEG	Hermann 2020	★	★		★	★★★
EEG	Lutkenhoff 2020	★	☆		★	★★
EEG	Martens 2020	★	★		★	★★★
EEG	Wang 2020	★	☆		★	★★
EEG	Zhang 2020	★	☆		★	★★
EEG	Liu 2021	★	☆		★	★★
EEG	Guo 2022	★	☆		★	★★
EEG	Han 2022	★	★		★	★★★
EEG	Han 2022	★	★		★	★★★
EEG	Visani 2022	★	★		★	★★★
EEG	Chen 2023	★	★		★	★★★
EEG	Maschke 2023	★	☆		★	★★
EEG	Rosenfelder 2023	★	★		★	★★★
EEG	Zhang 2023	★	★		★	★★★

Total score is on 7 points for studies including healthy controls and on 3 points for the other studies.